Ore Geology Reviews 122 (2020) 103525

Contents lists available at ScienceDirect

Ore Geology Reviews

journal homepage: www.elsevier.com/locate/oregeorev

Unique Cu-rich sulphide ores of the Southern-2 orebody in the Talnakh Intrusion, Noril'sk area (Russia): Geochemistry, mineralogy and conditions of crystallization

Nadezhda Tolstykh[a,b,*], Nadezhda Krivolutskaya[c], Inna Safonova[a,b], Mariya Shapovalova[a,b], Liudmila Zhitova[a,b], Adam Abersteiner[d]

[a] VS Sobolev Institute of Geology and Mineralogy, Siberian Branch Russian Academy of Sciences, Pr. Akademika Koptyuga, 3, Novosibirsk 630090, Russia
[b] Novosibirsk State University, Pirogova St. 2, Novosibirsk 630090, Russia
[c] Vernadsky Institute Geochemistry and Analytical Chemistry, Russian Academy of Sciences, 119991, Kosygina St., 19, Moscow, Russia
[d] School of Natural Sciences and Centre of Excellence in Ore Deposits (CODES), University of Tasmania, Hobart, Tasmania 7001, Australia

ARTICLE INFO

Keywords:
Cu-Ni ores
Southern-2 orebody
PGE
Minerals of platinum-group elements
Noril'sk region
Talnakh intrusion

ABSTRACT

We present new geochemical and mineralogical data from the Southern-2 orebody, located in the South-Western branch of the Talnakh intrusion (Russia) and composed of massive and disseminated sulphides. The Southern-2 orebody consists dominantly of chalcopyrite along with lesser pentlandite and subordinate cubanite, bornite and pyrrhotite, and differs from Cu-rich ores of the Oktyabr'sky deposit due to the absence of moikhukite-talnakhite assemblages. Ores from the Southern-2 orebody are highly enriched in copper, nickel and platinum-group elements (PGEs): Cu up to 28.12 and 10.58 wt%, Ni up to 6.29 and 2.45 wt%, and Pt + Pd up to 220 and 173 ppm in the massive and disseminated ores respectively. The ratios of Cu/Ni = 3.85–7.34 in massive and 2.64–6.58 in disseminated ores. The ratios of the platinum to iridium group elements (PPGE/IPGE) reaches more than 40000. These features indicate an extremely different degree of fractionation of the sulphide melt during the formation of ores. The sequence of crystallization of the PGE minerals (PGMs) on the basis of textural information was as follows: Pt-Pd-Sn (rustenburgite, atokite) → Pd-Cu-Sn (stannopalladinite) → Pt-Fe-Cu-Ni (tetraferroplatinum) → Pd-Ni-As (majakite) → Pd-As (palladoarsenide) → Pd-Pb(Bi) (zvyagintsevite, polarite and Pd_5Pb_3 unnamed phase) → Au-Cu-Pd (tetra-auricupride and auricupride) → Au-Ag alloys. This is consistent with experimental data on PGE minerals. The PGM assemblage was caused by the evolution of a significantly fractionated sulphide melt that was enriched in Cu, Ni, Pt, Pd, Pb and Au, and as a result produced minerals with peculiar compositions (e.g., Cu-rich stannopalladinite, Pb-rich polarite, Ni-rich palladoarsenide), which do not occur in other ores. Furthermore, Pt-Fe-Cu-Ni alloys are abundant and sperrylite is absent, which is a very common phase in all ores of the Noril'sk area. The composition of pentlandite with Ni/(Ni + Fe) ratios ranging from 0.48 to 0.68 indicates that it formed between 560 °C (Ni-poor) to 500 °C (Ni-rich) and −10.5 to −7 lgfS_2, respectively. The PGMs and Au-minerals were formed at temperatures ranging from 550 to 225 °C. The specificity of sulphide (with PGMs) association is due to the evolution of the Cu-rich (and Ni-rich) melt under elevated sulphur fugacity conditions. The mechanism of filter-pressing, which precipitated sulphide drops at the bottom of the chamber, and penetration of sulphide melts into the country rocks is supported by the same geochemical composition of disseminated and massive ores.

1. Introduction

The Noril'sk region is a world famous metallogenic province located in the Siberian platform (Russia) (Fig. 1). The Noril'sk sulphide ores are commercially unique compared to other world-class Cu-Ni-PGE deposits (Naldrett, 2004) due to their high concentrations of both Ni and platinum-group elements (PGEs). The large reserves of Ni and PGEs of the Noril'sk region are related to Early Triassic mafic–ultramafic igneous rocks of the Siberian Traps (e.g., Urvantsev, 1972). The Noril'sk-Talnakh deposits are unusual as they are comprised of large volumes of sulphide ores relative to the volume of intrusive silicate rocks, where the sulphide/silicate ratio can reach 0.18 (Likhachev, 1996; Lightfoot

* Corresponding author.
E-mail address: tolst@igm.nsc.ru (N. Tolstykh).

https://doi.org/10.1016/j.oregeorev.2020.103525
Received 26 December 2018; Received in revised form 10 March 2020; Accepted 6 April 2020
Available online 07 April 2020
0169-1368/

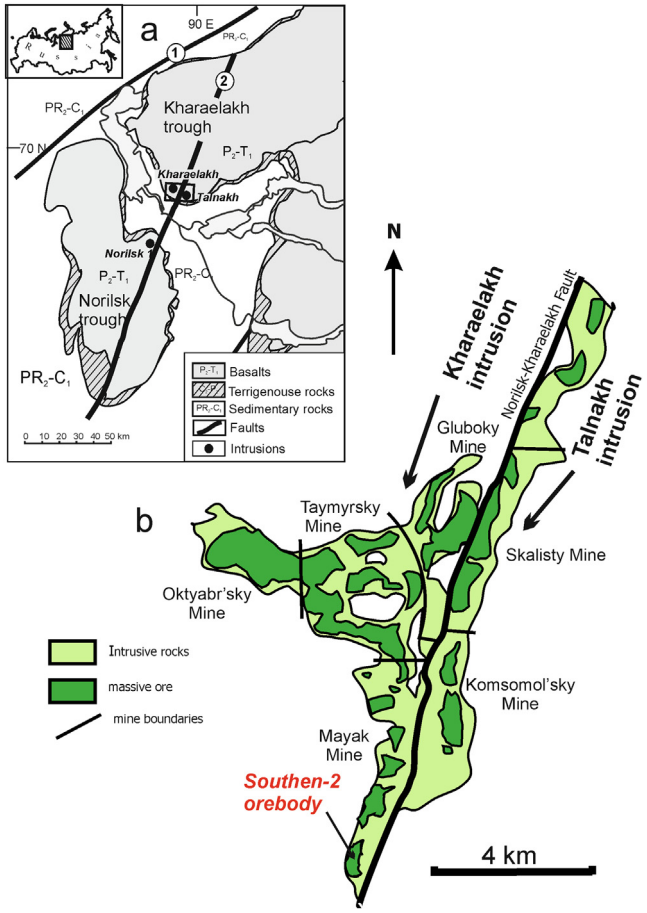

Fig. 1. Schematic geological map of the Noril'sk region: (a) position of the Talnakh and Kharaelakh intrusions and Southern-2 orebody (b), modified from Strunin (1991). (b) The sampling location. Faults: 1 – Yenisey-Khatangsky, 2 – Noril'sk-Kharaelakhsky.

and Zotov, 2014). The Noril'sk ores, their varieties, internal structure and mineral compositions, have been studied extensively (e.g., Kovalenker et al., 1972; Distler et al., 1975, 1996; Evstigneeva and Trubkin, 2006; Sluzhenikin and Mokhov, 2007, 2008, 2015; Dodin et al., 2009; Spiridonov, 2010 and other). The Noril'sk ores are characterized by a wide variety of minerals species (greater than400), in particular, platinum-group minerals (PGMs) (Genkin et al., 1966, 1969; Begizov et al., 1974; Razin and Borishanskaya, 1970; Evstigneeva and Genkin, 1983, 1990; Barkov et al., 2000a, 2000b, 2002). Many new minerals were first discovered in the Noril'sk area, including more than 50 PGMs and PGE-containing minerals (Sluzhenikin, 2011).

The massive ores are located on the exo- or endocontact between gabbro-dolerite and sedimentary country rocks (i.e. sandstone, limestone). The term exocontact is used to describe the sedimentary part of the contact zone between an igneous body and country rocks, whereas the endocontact is the magmatic part of the contact zone, which is located within the intrusion. Massive sulphides of Talnakh deposits are commonly localized within the exocontact (Likhachev, 2006).

The mechanisms of formation of large sulphide bodies in the exocontact zones remain open to debate. They were formed either as a result of the intrusion of multiple independent injections of sulphide melt (Stekhin, 1994; Distler et al., 1988, Dyuzhikov et al., 1988) or the result of filter pressing processes (Likhachev, 1996, 2006), which occurred when the sulphide melt penetrated into structural traps. These structural traps appear to be important sites for the accumulation of sulphides (Barnes and Lightfoot, 2005). Other studies suggested that those ores can be derived by emplacement of a sulphide melt (Genkin et al., 1981; Distler et al., 1988; Lightfoot and Zotov, 2014). Others support the idea that sulphides were transported by the magma as small drops from a mantle (or lower-crustal) source enriched in heavy S isotopes (Likhachev, 2006; Krivolutskaya, 2014), such as those described at Voisey's Bay (Labrador, Canada) and Jinchuan deposit in Northwest China (Lightfoot et al., 2012).

There is a generally accepted crystallization model for the formation of Fe-rich (pyrrhotite) and Cu-rich (chalcopyrite) ores, based on experimental studies. The main model reflects a continuous process of crystallization differentiation of the sulphide melt, when a Fe-rich monosulphide solid-solution (MSS) cumulate and a Cu-rich sulphide liquid enriched with incompatible elements which later crystallized as an intermediate solid solution (ISS) (Kullerud et al., 1969; Naldrett, 2004; Sinyakova and Kosyakov, 2009; Barnes and Ripley, 2016; Duran et al., 2017). The Cu-rich sulphide liquid appears to have migrated from MSS in the footwall to form veins that extend into the country rock or forms a superimposed impregnation over the ore body (Naldrett, 2004). In addition, there is another liquation-crystallization model that includes the segregation of the sulphide melt at the pre-crystallization stage into Cu- rich and Fe-rich liquids, which then evolved separately (Likhachev, 2006; Genkin et al., 1981; Distler et al., 1975). Both of these models are recognised in the Noril'sk deposits and explain the different types of ore zoning. The zoning of the first type is simple (i.e. from pyrrhotite to chalcopyrite), where as the second type of zoning is complex and 'jump-like'. This reflects various trends and includes sulphur undersaturated talnakhite and moikhukite (Distler et al., 1975).

Detailed studies of ore mineralogy were performed on the Oktyabr'sky deposit, which is the main orebody to exhibit a strongly zoned structure (Genkin, 1968; Sukhanova, 1968; Dodin et al., 1971; Genkin et al., 1981; Distler et al., 1988; Distler and Kunilov, 1994; Likhachev, 1994; Naldrett et al., 1996). The zoning of the ore body is related to the change of sulphide parageneses (ore types) as a result of in-situ fractionation of the sulphide melt in the magma chamber (Distler et al., 1975).

The Southern-2 orebody was first studied by Noril'sk geologists in the early 1970s. It is enriched in copper (Sluzhenikin et al., 2014) and consists predominantly of chalcopyrite, which contrasts with other parts of the Talnakh intrusion that are dominated by pyrrhotite. The aim of this work is to identify the mineralogical and geochemical features of this ore body in order to understand different aspects of its genesis and the reasons for the differences between the Southern-2 orebody from other ore bodies of the Noril'sk region. New data on the structure of the South-Western branch of the Talnakh intrusion and the Southern-2 orebody was recently presented by Krivolutskaya et al. (2018). Special emphasis was placed on documenting and understanding the mineral compositions of sulphides and PGMs as indicators of mineralization conditions, geochemical characteristics of the ores, PGM parageneses, conditions and succession of PGM crystallization as well as comparison to other ore bodies of the Noril'sk region.

2. Geological background

The Noril'sk region of Russia is located in the north-western part of Siberian Platform at its junction with the Yenisei-Khatanga troughs and the Tunguska syncline. The intrusions were emplaced in sedimentary sequences (coal-bearing terrigenous sediments, evaporites, carbonates) of the different ages, ranging from Devonian to Upper Permian and the lowest trap basalt formations (Naldrett, 2004; Sluzhenikin et al., 2014; Krivolutskaya, 2014) (Fig. 1). Numerous ultramafic–mafic sills and dikes are typically hosted in the sedimentary rocks. Several intrusions (Noril'sk 1, Noril'sk 2, Maslovsky) are hosted by the lower part of volcanic sequences in the Ivakinsky-Nadezhdinsky formations (Strunin, 1991; Krivolutskaya and Rudakova, 2009; Krivolutskaya et al., 2012). These intrusions are differentiated and contain economic ore deposits.

The major intrusions of the Noril'sk region (Kharayelakh, Talnakh and Noril'sk 1) host large bodies of disseminated and massive sulphide

ores. The Kharayelakh and Talnakh intrusions are located in the southern part of the Kharayelakh trough and are separated by the Noril'sk-Kharayelakh Fault (N-K) (Fig. 1). They were either once a single body which was later separated by the fault into two parts (Dodin et al., 1971; Genkin et al., 1981), or they were formed separately along the N-K Fault (Likhachev, 1996). The two intrusions have similar internal structure and rock compositions, but they exhibit differences in the compositions of the ores, in particular, the massive ores. The Kharayelakh intrusion comprises of many ore bodies, including the large Oktyabr'sky sulphide deposit (around 2 × 4 × 0.05 km). This orebody has a zoned structure: the central part is enriched in copper and composed of talnakhite and mooihoekite, the intermediate part consists of cubanite, and the peripheral parts are dominated by pyrrhotite. The smaller ore bodies of the Kharayelakh intrusion are dominated by pyrrhotite and/or chalcopyrite.

The Talnakh intrusion consists of two branches: the North-Eastern and South-Western. The South-Western branch (Mayak Mine) is bounded by a fracture zone aligned along the Noril'sk-Kharaelakh fault (Genkin et al., 1981) (Fig. 1). The intrusion includes several N-S-striking ore bodies. The massive ores are concentrated close to the bottom of the intrusion, several tens of centimetres to several meters away from the contact with the Devonian carbonate-terrigenous sedimentary country rocks (Fig. 2). The contact zone is typically < 1 m thick and shows a gradual transition from moderately to highly disseminated sulphide mineralization at the exocontact to massive sulphide ores at the endocontact, as documented in borehole OUG-2 (Sluzhenikin et al., 2014). The massive sulphide ores of the north-eastern branch of the Talnakh intrusion (Skalisty and Komsomolsky Mines) are dominated by pyrrhotite with subordinate chalcopyrite and other sulphides. The Southern-2 orebody is located in the south-western branch of the Talnakh Intrusion (Fig. 1). The layer-shaped and extended orebody is hosted by gabbro-dolerites (mostly in taxitic gabbro-dolerites, Fig. 2b) and occur along the contact with the Devonian carbonate-sulphate-terrigenous rocks of the Kalargonsky Formation and late Carboniferous - middle Permian terrigenous rocks of the Tunguska Group (Fig. 2). The samples for this study were selected from the “Mayak” mine and from boreholes intersecting the Southern-2 orebody (Fig. 2).

3. Analytical methods and techniques

Five ore samples from Mayak mine of 37 m horizon were analysed for all six PGEs, Au and base metals (BM). The concentrations of BM (Fe, Cu, Ni, Co) in whole rock samples were determined with an S4 Pioneer X-ray spectrometer (semi-quantitative XRF) at the Vinogradov Institute of Geochemistry SB RAS, Irkutsk. The analytical technique used to determine platinum-group elements (PGEs) Ru, Rh, Pd, Ir and Pt as well as Au in the geological samples within 0.1 ppb–10 ppm range and Os on ppb level in the ultramafic rocks by inductively coupled plasma mass-spectrometry (LA-ICPMS) with external calibration and without chemical removal of main interferences of Zr and Hf. The samples were prepared after their decomposition by acid in the open vessels and melting the insoluble residue with NH4F, and with a subsequent cation exchange separation of PGEs from matrix elements by KU-2-8 resin (Russia). Measurements were carried out using the high resolution mass-spectrometer Element 2 (Germany). The accuracy of the technique on ppm level was verified with reference materials: pyrrhotite ore (RP-1) and sulphide copper-nickel ore (Zh-3). In addition, the accuracy of the trace level (ppb) has been verified by comparing the results obtained by this study with those reported in the literature for sample OPY-1, developed by the International Association

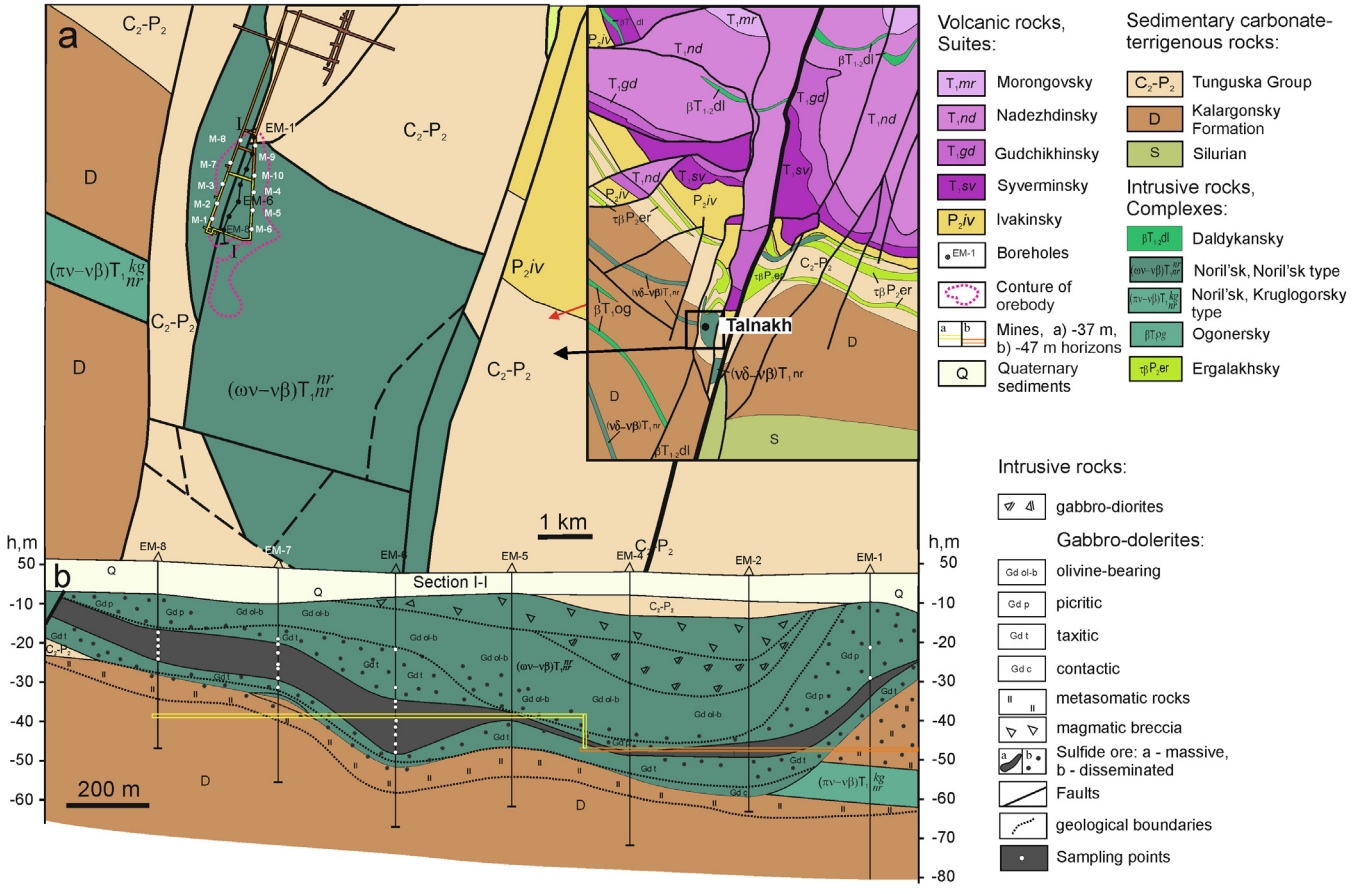

Fig. 2. Schematic geological map of the southern part of the Talnakh deposit (a) and cross-section through the Southern-2 orebody (b). Modified from Ltd. Noril'skGeology materials.

of Geoanalysts (IAG). The procedural blanks are: 0.00023 ppb for Os and Ru, 0.0016 ppb for Ir and Rh, 0.026 ppb for Pd, 0.018 ppb for Pt. The detection limits were estimated taking into account the blanks and their standard deviations and were (ppb): 0.02 for Os, 0.09 for Rh and Ir, 0.13 for Ru, 1.0 for Pt and 1.4 for Pd, respectively (Men'shikov et al., 2016).

In addition, 22 samples of massive and disseminated ores from boreholes (EM-1, EM-6, EM-7 and EM-8) were analysed for Pt, Pd, Au and BM. In this case, base and precious metals were analysed at the Laboratory of the Geochemistry and Analytical Chemistry of Precious Metals at the Vernadsky Institute of Geochemistry and Analytical chemistry of RAS (analysts I.V. Kubrakova and O.A. Tyutyunnik). To analyse ore samples for pressure metals, they were decomposed by heating to 120 °C in mixture of strong HF + HNO_3 and then dried to wet salt. The salt was treated using aqua regia to completely oxidize elementary sulphur, where wet salts were then obtained. Upon the complete dissolution of the salts, the solution was cooled and filtered into a 100 mL flask. The filter with precipitate was placed into a corundum crucible, reduced to ash in a muffle furnace at 500 °C, and then fused with a double-excess amount of Na_2O_2 at 600 °C. The bead was then treated in compliance with conventionally used procedures to convert the salts into chlorides. The solution was mixed with a filtrate in the flask. To analyse Au, Pt and Pd, preparatory concentration on a POLIORGS IV was performed, and the suspension was then analysed by ETAAS on a SolaarMQZ (ThermoElectron Corpration, UK) using a wavelength of 242.8, 265.9 and 247.6 nm, detection limited are 1 ppb for Pd and Au and 2 pmm for Pt. Fe, Cu, Ni, Co, and S were analysed by ICP-AES on an Iris Intrepid II XDL (ThermoElectron Corporation, USA). The accuracy of the analyses was controlled by replicate analysis of standard reference samples SARM-7B (Pt ore) and KN-1 (NI concentrate).

The sulphide minerals and PGMs were investigated from different parts of the Mayak Mine (37 m horizon). PGM grains were selected from six ore samples (approximately 0.5–0.7 kg each) after crushing and gravitational concentration using heavy liquids. The polished sections of ores were studied with an Axio A1 microscope. The chemical compositions of the minerals were examined at the analytical centre for multi-elemental and isotope research of the VS Sobolev Institute of Geology and Mineralogy SB RAS (IGM SB RAS). The energy-dispersive spectroscopic (EDS) analyses were carried out using scanning-electron microscope (SEM) LEO 1413 VP at an accelerating voltage of 20 kV, a probe current of 1.6nA, an accumulation time of 50 s and beam size of < 0.1 μm. The following standards were used: pyrite (S), $PtAs_2$ (As), HgTe (Te), metallic Zn, Co, Ni, Cu, Ru, Rh, Pd, Ag, Sn, Sb, Os, Ir, Pt, Au etc. The detection limit for most elements is 0.2–0.3% (3 sigma criterion), but in some cases it can be as high as 0.5–0.8% in the case of peak overlaps or using the L line for analyses of heavy (Z > 72) elements. Correction for matrix effects was done using the XPP algorithm.

The WDS analyses of BMSS and PGMs were carried out using a "Camebax-Micro" microprobe (~1-mm beam) at 20 kV voltage, 20–30 mA current and 10 s duration of measurement for each analytical line. The following standards were used: pure metals for Pt, Pd, Rh, Os, Ir, Ru, Te, Au and Ag, Cu, Ni and Fe (during the analysis of PGMs and Pt-Fe and Au-Pd-Cu alloys); synthetic compounds $CuFeS_2$ for Cu, FeS_2 for Fe and S, NiAs for As and Ni, FeNiCo for Co, Bi_2S_3 for Bi, PbS for Pb, and SnTe for Sn. The following X-ray lines were selected: Lα for Pt, Pd, Rh, Ag, Ir, Ru, Te, Sn, and As; Kα for S, Fe, Cu, Ni, and Co; Mα for Au, Bi, Os and Pb. Overlapping elements in the X-ray spectra were corrected with the assistance of a program, including experimentally calculated coefficients (Lavrentyev and Usova, 1994). The accuracy and reproducibility of analytical procedures and comparison of WDS with EDS data were evaluated with special tests (Korolyuk et al., 2009; Lavrent'ev et al., 2015a, 2015b). All of the data in the tables are listed according to the detection limits of the elements (Table 1).

Table 1
Detection limits for elements analysed during the study of mineral chemistry, performed by the "Camebax" microprobe (wt.%).

Element	wt.%	Element	wt.%
Os	0.06	Cu	0.06
Ir	0.17	Ni	0.05
Ru	0.04	Co	0.03
Rh	0.04	As	0.08
Pt	0.2	Te	0.04
Pd	0.04	Bi	0.06
Au	0.06	Pb	0.09
Ag	0.04	S	0.01
Fe	0.03	Sn	0.03

4. Chemical composition of the Southern-2 orebody

4.1. Massive ore

All massive ore samples are enriched in copper, which has concentrations ranging from 15.60 to 28.12 wt% (average 23.39). The concentrations of Ni are also very high, varying from 2.36 to 6.29 wt% (average 4.43) (Table 2). Copper is greater than nickel in all studied samples where the Cu/Ni ratio in the samples varies from 3.85 to 7.34 (average 5.27) (Table 3). The ores in this study are characterized by the highest absolute concentrations of Cu (up to 28.12 wt%) and Ni (up to 6.29 wt%), but the Cu/Ni ratio is close to that of the copper-rich ores of Noril'sk 1 deposit (Naldrett, 2004; Duran et al., 2017). The concentration of Pt + Pd in massive ores varies from 36.24 to 220.33 ppm (103.54 on average). The analyses of the massive ores have similar values to those calculated to 100% sulphides (Table 2). Massive sulphide ores from mines (yuz-5 - yuz-12) represent almost pure crystallized sulphide melt, in which the content of silicates and oxides is < 1–3 wt%. Only the refractory PGEs (IPGE = Os + Ir + Ru) analysed in the mine ores are very low (2.40–12.50 ppb; average 6.90) (Table 2). The concentrations of Au in massive ores ranges from 1.39 to 9.91 ppm (average 5.0) and have a positive correlation with PGEs (Fig. 3a), while the correlation of PGEs with sulphur was not observed in the massive ores (Fig. 3b). The concentrations of Co and Ni in the vein-disseminated ore of the upper part of the ore body are two times lower in comparison with massive ores, whereas the content of Au is very high (Fig. 3a) and PGEs reach 173.28 ppm (Table 2).

Strong fractionation of elements in massive ore is reflected in the chondrite-normalized PGE patterns (Tagle and Berlin, 2008) which show a clear negative anomaly in IPGEs and strong enrichment in Pd, Au and Cu (Fig. 4). The concentrations of Rh are close to chondritic. The concentration of Pt varies over a wider range than the concentration of Pd. Pt-rich and Pt-poor samples are controlled by the ratio of Pt- and Pd-minerals in the samples. In general, the concentrations of PGEs in 100% sulphide phase increase with Cu + Ni content. In the pf PGEs versus (Cu + Ni) diagram (Fig. 5a), the samples from this study extend the trend of the Oktyabr'sky (Noril'sk 1), and Talnakh ores (Naldrett, 2004).

4.2. Disseminated ore

The host rocks (picritic and taxitic gabbro-dolerite) also contain disseminated PGE-bearing sulphide mineralization above the massive ore body. The concentration of Pt + Pd in disseminated and vein-disseminated ores varies from 13.94 to 169.70 ppm (84.40 in average) (Table 3), and is positively correlated with the sulphur content, whereas there is no similar correlation in massive ores (Fig. 3b). The concentrations of PGE in picritic gabbro-dolerite are greater than that of taxitic gabbro-dolerite (Table 2), but the values of Pd/Pt are similar (Table 3). The concentrations of Cu and Ni in disseminated ores correlate with the amount of sulphur. However, the ratio of Cu/Ni varies

Table 2
Composition of sulphide ores from the Southern-2 orebody of the Talnakh intrusion.

No.	Ore type	Sample	Cu	Ni	Co	S	Pt	Pd	Au	Rh	Ir	Os	Ru
			wt .%				ppm				ppb		
1	massive ore (mine)	Yuz/5	21.93	5.70	0.17	35.39	38.58	89.07	4.97	0.15	2.20	7.50	2.80
2	massive ore (mine)	Yuz/7	19.36	3.98	0.14	36.38	1.12	50.71	1.30	0.07	2.40	4.50	2.80
3	massive ore (mine)	Yuz/10	23.45	4.09	0.13	35.93	0.19	64.49	1.60	0.05	2.80	0.10	2.30
4	massive ore (mine)	Yuz/11	23.66	4.15	0.12	35.64	0.51	65.33	1.37	0.05	1.30	0.10	1.00
5	massive ore (mine)	Yuz/12	23.34	4.53	0.12	34.73	62.35	157.98	3.87	0.06	1.90	0.70	2.30
6	massive ore (borehole)	EM6_90	24.50	4.79	0.07	29.82	37.56	117.78	5.60				
7	massive ore (borehole)	EM6_92.5	25.17	5.02	0.06	31.24	2.72	33.52	1.23				
8	massive ore (borehole)	EM6_94	23.60	3.87	0.07	33.21	47.19	128.18	7.20				
9	massive ore (borehole)	EM6_96.5	17.25	4.22	0.13	32.15	36.57	78.14	6.00				
10	massive ore (borehole)	EM6_98.4	26.12	5.22	0.07	33.19	27.59	87.82	9.30				
11	massive ore (borehole)	EM7_70.1	21.90	3.94	0.07	31.50	19.02	87.32	5.70				
12	massive ore (borehole)	EM7_72	26.70	5.98	0.07	32.05	10.09	71.13	6.10				
13	massive ore (borehole)	EM7_73.8	26.40	6.29	0.08	32.40	11.35	84.45	4.00				
14	massive ore (borehole)	EM7_76	27.80	4.31	0.07	31.30	24.79	82.80	5.60				
15	massive ore (borehole)	EM7_77	22.90	3.12	0.06	27.40	20.68	70.48	3.80				
16	massive ore (borehole)	EM8_68.5	27.33	3.96	0.07	31.45	17.4	81.11	8.94				
17	massive ore (borehole)	EM8_70	28.12	4.01	0.06	32.20	14.1	84.01	4.80				
18	massive ore (borehole)	EM8_72	27.14	6.13	0.07	33.20	8.7	75.70	7.88				
19	massive ore (borehole)	EM8_74.3	26.30	4.86	0.07	31.70	16.4	81.08	2.84				
20	massive ore (borehole)	EM8_75.5	23.30	4.27	0.07	32.20	16.4	66.50	7.83				
21	vein-disseminated ore	EM6_85	12.66	2.36	0.02	16.02	29.60	73.89	10.88				
22	vein-disseminated ore	EM6_87.5	15.60	2.76	0.03	17.19	38.17	135.11	6.90				
23	picritic gabbro-dolerite	EM1_71	6.48	2.45	0.01	6.76	24.95	58.67	3.37				
24	picritic gabbro-dolerite	EM1_82.5	10.58	1.98	0.01	10.15	75.87	93.92	5.90				
25	taxitic gabbro-dolerite	EM6_71	2.78	0.58	0.02	3.19	3.31	10.63	0.85				
26	taxitic gabbro-dolerite	EM6_81	3.93	0.77	0.01	4.53	8.86	22.56	2.44				
27	taxitic gabbro-dolerite	EM7_69	7.17	1.09	0.02	4.28	3.7	11.72	0.79				
Concentrations of ore elements calculated on 100% sulphide*													
No	Ore type	Sample	Cu	Ni	Co	S	Pt	Pd	Au	Rh	Ir	Os	Ru
1	massive ore (mine)	Yuz/5	22.05	5.73	0.17	35.58	38.79	89.55	4.99	0.15	2.21	7.54	2.81
2	massive ore (mine)	Yuz/7	19.53	4.01	0.14	36.70	1.13	51.16	1.31	0.07	2.42	4.54	2.82
3	massive ore (mine)	Yuz/10	23.44	4.09	0.13	35.91	0.19	64.46	1.60	0.05	2.80	0.10	2.30
4	massive ore (mine)	Yuz/11	23.78	4.17	0.12	35.83	0.51	65.68	1.38	0.05	1.31	0.10	1.01
5	massive ore (mine)	Yuz/12	23.94	4.65	0.12	35.63	63.96	162.07	3.97	0.06	1.95	0.72	2.36
6	massive ore (borehole)	EM6_90	28.65	5.60	0.08	34.87	43.92	137.73	6.55				
7	massive ore (borehole)	EM6_92.5	28.15	5.61	0.07	34.94	3.04	37.49	1.38				
8	massive ore (borehole)	EM6_94	25.31	4.15	0.07	35.62	50.62	137.49	7.72				
9	massive ore (borehole)	EM6_96.5	19.49	4.77	0.14	36.33	41.32	88.29	6.78				
10	massive ore (borehole)	EM6_98.4	27.58	5.51	0.07	35.04	29.13	92.71	9.82				
11	massive ore (borehole)	EM7_70.1	24.78	4.46	0.08	35.64	21.52	98.79	6.43				
12	massive ore (borehole)	EM7_72	28.88	6.47	0.08	34.67	10.92	76.94	6.62				
13	massive ore (borehole)	EM7_73.8	28.28	6.74	0.08	34.70	12.15	90.46	4.30				
14	massive ore (borehole)	EM7_76	30.84	4.78	0.08	34.72	27.50	91.84	6.26				
15	massive ore (borehole)	EM7_77	29.32	3.99	0.08	35.08	26.48	90.25	4.87				
16	massive ore (borehole)	EM8_68.5	30.30	4.39	0.07	34.87	19.31	89.93	9.91				
17	massive ore (borehole)	EM8_70	30.44	4.34	0.07	34.86	15.32	90.94	5.20				
18	massive ore (borehole)	EM8_72	28.41	6.42	0.08	34.75	9.06	79.23	8.25				
19	massive ore (borehole)	EM8_74.3	28.94	5.35	0.08	34.88	18.07	89.21	3.12				
20	massive ore (borehole)	EM8_75.5	25.66	4.70	0.08	35.47	18.08	73.24	8.63				
21	vein-disseminated ore	EM6_85	27.92	5.21	0.04	35.33	65.29	162.98	24.00				
22	vein-disseminated ore	EM6_87.5	31.61	5.59	0.06	34.83	77.34	273.74	13.98				
23	picritic gabbro-dolerite	EM1_71	32.17	12.16	0.04	33.56	123.87	291.26	16.72				
24	picritic gabbro-dolerite	EM1_82.5	35.34	6.61	0.02	33.91	253.45	313.77	19.74				
25	taxitic gabbro-dolerite	EM6_71	30.36	6.33	0.18	34.83	36.19	116.07	9.27				
26	taxitic gabbro-dolerite	EM6_81	30.33	5.94	0.08	34.96	68.35	174.13	18.83				
27	taxitic gabbro-dolerite	EM7_69	54.06	8.22	0.14	32.27	27.61	88.34	5.93				

Note. * Calculation method described in Barnes and Lightfoot, 2005; EM6_90 – borehole number and depth.

from 2.64 to 6.58 (4.90 average), which is comparable with massive ores of Southern-2 orebody (Cu/Ni is 5.27) (Table 2), and at the same time differs from disseminated sulphides of the Noril'sk 1 (1.95) and Talnakh (1.68) intrusions (Duran et al., 2017). Chondrite-normalized PGE patterns (Tagle and Berlin, 2008) in disseminated ores show also a similar distribution of analysed elements as in massive ores (Fig. 4).

The following geochemical features were noted: (1) a steep positive slope in the chondrite-normalized PGE patterns, which is due a high degree of fractionation of elements both in massive and in disseminated ores; (2) Cu/Ni ratios in massive and disseminated ores have similar values; (3) the concentrations of PGEs in disseminated (in 100% sulphide) prevails over those of massive ores; (4) the concentrations of PGEs in picritic gabbro-dolerites prevails over those in taxitic gabbro-dolerites (Table 3); (5) both massive and disseminated ores of Southern-2 orebody are characterized by higher concentrations of ore elements compared to those previously published for the Noril'sk-Talnakh ores (Naldrett, 2004) and continue the trend of compositions on the Pt + Pd versus Cu + Ni diagram (Fig. 5).

5. Mineralogical composition of the Southern-2 orebody

5.1. Sulphide minerals

The mineralogy of samples from massive ores only taken from the

Table 3
Characteristics of sulphide ores from the Southern-2 orebody in the Talnakh intrusion.

No	Ore type	Sample	Σ PGE (ppm)	Pd/Pt	Cu/Ni	Ni/Cu	Cu/Pd	PPGE/IPGE	Ni/Ir
1	massive ore (mine)	Yuz/5	127.81	2.31	3.85	0.26	2462	10224	25909091
2	massive ore (mine)	Yuz/7	51.91	45.28	4.86	0.21	3818	5351	16583333
3	massive ore (mine)	Yuz/10	64.74	339.42	5.73	0.17	3636	12448	14607143
4	massive ore (mine)	Yuz/11	65.89	128.10	5.70	0.18	3622	27453	31923077
5	massive ore (mine)	Yuz/12	220.38	2.53	5.15	0.19	1477	44975	23842105
6	massive ore (borehole)	EM6_90	155.34	3.14	5.11	0.20	2080		
7	massive ore (borehole)	EM6_92.5	36.24	12.32	5.01	0.20	7509		
8	massive ore (borehole)	EM6_94	175.37	2.72	6.10	0.16	1841		
9	massive ore (borehole)	EM6_96.5	114.71	2.14	4.09	0.25	2208		
10	massive ore (borehole)	EM6_98.4	115.41	3.18	5.00	0.20	2974		
11	massive ore (borehole)	EM7_70.1	106.34	4.59	5.56	0.18	2508		
12	massive ore (borehole)	EM7_72	81.22	7.05	4.46	0.22	3754		
13	massive ore (borehole)	EM7_73.8	95.80	7.44	4.20	0.24	3126		
14	massive ore (borehole)	EM7_76	107.59	3.34	6.45	0.16	3357		
15	massive ore (borehole)	EM7_77	91.16	3.41	7.34	0.14	3249		
16	massive ore (borehole)	EM8_68.5	98.51	4.66	6.90	0.15	3369		
17	massive ore (borehole)	EM8_70	98.11	5.96	7.01	0.14	3347		
18	massive ore (borehole)	EM8_72	84.40	8.70	4.43	0.23	3585		
19	massive ore (borehole)	EM8_74.3	97.48	4.94	5.41	0.19	3244		
20	massive ore (borehole)	EM8_75.5	82.90	4.05	5.46	0.18	3504		
21	vein-disseminated ore	EM6_85	103.49	2.50	5.36	0.19	1713		
22	vein-disseminated ore	EM6_87.5	173.28	3.54	5.65	0.18	1155		
	Disseminated ores in gabbro-dolerite (gd)								
23	picritic gd (borehole)	EM1_71	83.62	2.35	2.64	0.38	1104		
24	picritic gd (borehole)	EM1_82.5	169.79	1.24	5.34	0.19	1126		
25	taxitic gd (borehole)	EM6_71	13.94	3.21	4.79	0.21	2615		
26	taxitic gd (borehole)	EM6_81	31.42	2.55	5.10	0.20	1742		
27	taxitic gd (borehole)	EM7_69	15.42	3.17	6.58	0.15	6118		

Mayak mine of the Southern-2 orebody were analysed (horizon 37 m, Fig. 2). The sulphide ores of the Southern-2 orebody are dominated by chalcopyrite and, to a lesser extent, by pentlandite, cubanite, bornite and pyrrhotite (Figs. 6–8). The amount of pyrrhotite is insignificant and exhibits only minor increases in the lower part of the ore body. Chalcopyrite hosts lamellae of exsolved cubanite (Fig. 7a, b). Pentlandite forms granular, lenticular and belt segregations in cubanite (Fig. 7c) and chalcopyrite (Fig. 7d, e). PGMs are always hosted by chalcopyrite (Fig. 7f).

The Fe/S ratio in pyrrhotite varies from 0.87 to 0.90 (i.e. the formula is $Fe_{0.87}S_{1.00}$) and the concentration of Ni in pyrrhotite is low (less 0.1 wt%) (Table 4). Pentlandite is Ni-rich, where Ni content ranges from 31.83 to 46.29 wt% (35.5 average) and the Ni units in the mineral formula range from 4.31 to 6.12 (Table 4; Fig. 8a). The (Fe + Co)/Ni ratio in pentlandite varies from 0.51 to 1.05. Pentlandite contains ubiquitous Co (0.39–0.57 wt%) and sporadic Cu (0.06–0.35 wt%), where the concentration of Cu increases with increasing Ni (Table 4). The Me/S ratio (Me = Ni + Fe + Co + Cu) in studied pentlandite varies from 1.10 to 1.14. There is a negative correlation between Ni and S (-0.44). The formula is $Me_{9-x}S_8$ for Ni-rich pentlandite, and $Me_{9+x}S_8$ – for Fe-rich pentlandite. This is in agreement with the crystal chemistry features of other natural pentlandites (Rajamani and Prewitt, 1973; Likhachev, 2006).

The compositions of chalcopyrite and cubanite match and have ideal formulas (Table 4). In the Fe-Cu-S triangle, bornite plots in a tight field (Fig. 8b) and is characterized by a deficiency in Fe and S, and excess of Cu compared to its ideal formula. Bornite of this composition is sometimes called “pink” (Godovikov, 1997) and is a magmatic mineral unlike Cu-poor bornite (“orange” or X-bornite), which is exogenic (Gablina, 2008). Millerite is less abundant and was found in a sample with the most Ni-enriched pentlandite (Table 4, Fig. 8a) and is consistent with previous observations (Distler et al., 1975).

5.2. *Platinum-group minerals*

A total of 11 species of PGMs (306 grains) and Au-Ag-Cu-Pd

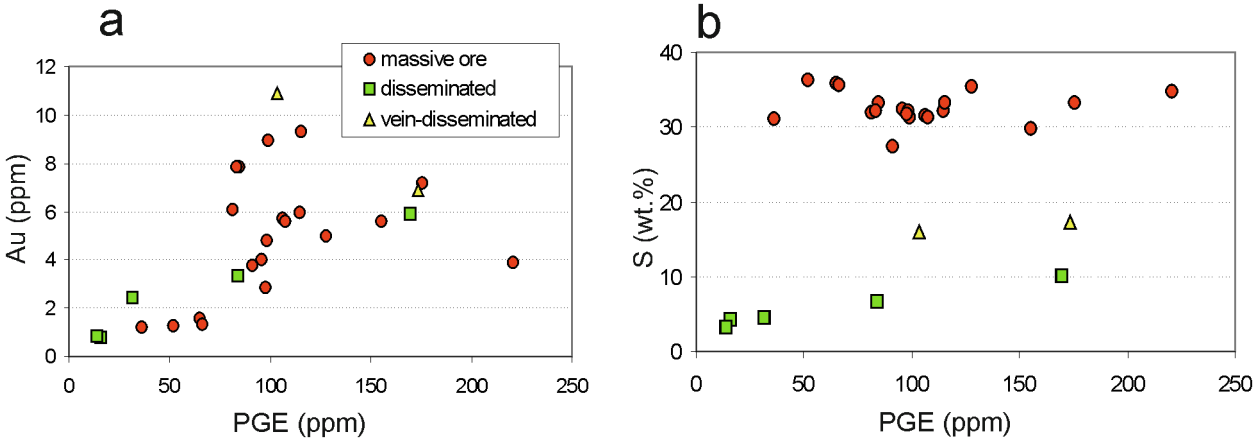

Fig. 3. Binary diagrams: PGE versus Au (a), PGE versus S (b).

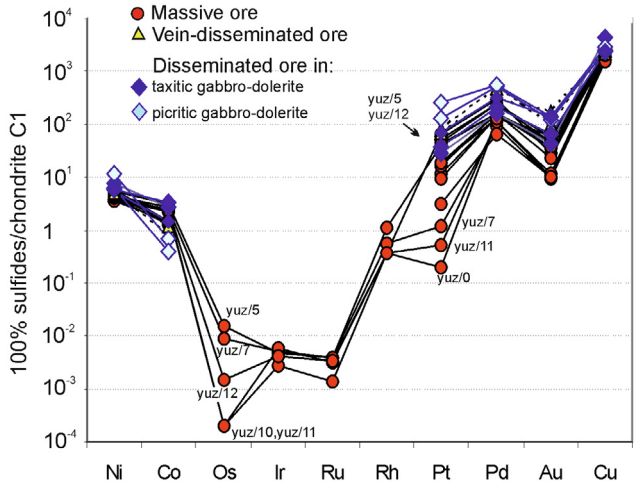

Fig. 4. Chondrite-normalized PGE patterns of various ore types of the Southern-2 Orebody by (Tagle and Berlin, 2008).

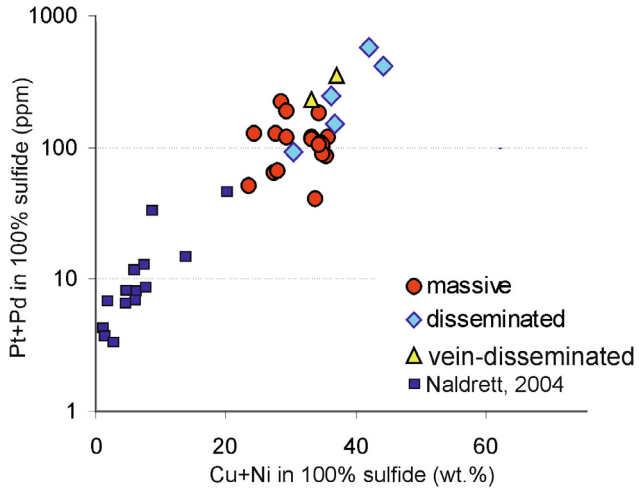

Fig. 5. Σ Pt + Pd compositions in the ores (ppm) versus Σ Cu + Ni (wt.%) of the Southern-2 orebody compared to the compositions of different types of Cu-Ni ores of Noril'sk region (Naldrett, 2004).

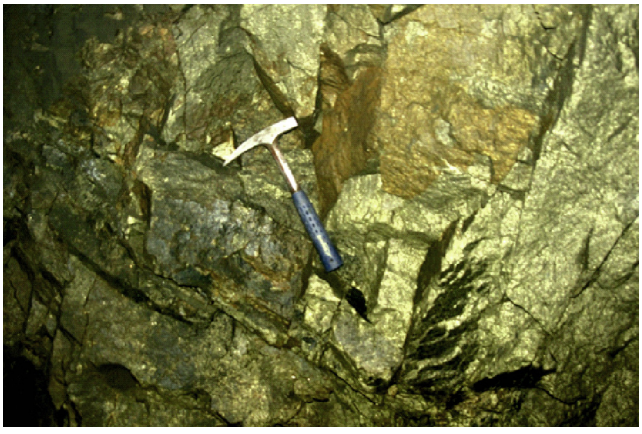

Fig. 6. Massive chalcopyrite ore of the Southern-2 orebody, Mayak mine (horizon 37 m).

minerals (62 grains) are intergrown with each other (Figs. 9, 10), and among them are minerals of the Pd(Pt)-Cu-Sn system, which predominates (35%) by the number of grains (grain size is not counted): stannopalladinite, rustenburgite, atokite and taimyrite (Fig. 9a). The minerals of the Pd-Pb(Bi) system (polarite, zvyagintsevite, plyumbopalladinite and unnamed Pd_5Pb_3) are second in prevalence (23%). Tetraferroplatinum is makes up 16% of the all minerals containing precious metals. Less common (7%) are minerals of Pd-Ni-As system (majakite, palladoarsenide, stillwaterite and unnamed Pd_3As, $(Pd,Ni)_5As_2$, $(Ni,Pd)_5As_2$) phases. The minerals of Au-Ag-Cu-Pd: (Au-Ag alloys, auricupride and tetra-auricupride) in intergrowths with PGMs are also very common (18%). Most these minerals are found in all studied samples, but the differences in their proportions are insignificant (Fig. 9b, c). However, tetraferroplatinum is more widespread in samples with Pd/Pt values < 3 (yuz/5,yuz/12). In addition, the number of grains of Pd minerals remains practically unchanged (Fig. 9a, b). The majority of PGMs (86%) are intergrown with chalcopyrite, and the remaining (14%) are associated with pentlandite. The Pt-Ni-Fe alloys only are intergrown with both chalcopyrite (Fig. 7f) and pentlandite (Fig. 10d, e). All PGMs are associated with chalcopyrite and only Pt-Fe-Ni-Cu alloys and stannopalladinite are associated with pentlandite. Pyrrhotite presents in small amounts in the ores and is not found in intergrowths with PGMs.

5.2.1. *Intermetallic compounds of the Pt-Fe-Cu-Ni system*

Platinum-iron-copper-nickel alloys were found in all studied samples as sporadic discrete grains, aggregates, ribbon-shaped grains, and bordering on aggregates of stannopalladinite and pentlandite (Fig. 10a–e). Au-Cu-Ag alloys often occur as rims around the nodules of Pt-Fe-Ni-Cu alloys (Fig. 10e). However, Au-Ag alloys are most often found as intergrowths with stannopalladinite. Compositionally, the intermetallics of Pt-Fe-Cu-Ni belong to the Cu- and Ni-bearing tetraferroplatinum or tetraferroplatinum-tulameenite-ferronickelplatinum solid solutions. Tetraferroplatinum contains Pd (1.14–1.22 wt%) and Rh (0.04–0.12 wt%) as minor elements (Table 5). The compositions of Pt-Fe-Ni-Cu alloys of the Southern-2 orebody and of the Noril'sk-Talnakh ores in general vary within a narrow range (Genkin and Evstigneeva, 1986; Sluzhenikin et al., 1994; Distler et al., 1999; Cook et al., 2002; Komarova et al., 2002; Kozyrev et al., 2002; Spiridonov et al., 2003, 2004) (Fig. 11a).

5.2.2. *Minerals of the Pd-Ni-As system*

The minerals of the Pd-Ni-As system are majakite, palladoarsenide, stillwaterite, and several other unnamed minerals. The mineral majakite was first discovered at the Mayak mine (Genkin et al., 1976) and in English it is translated to “majakite” (Cabri, 2002) (PdNiAs). It occurs as subhedral crystals 40–50 μm in size in association with stannopalladinite, polarite, tetra-auricupride and Au-Ag alloys (Fig. 10f–h). Majakite has been previously discovered in both the Noril'sk 1 and Talnakh deposits (e.g., Genkin et al., 1976, 1981; Komarova et al., 2002; Kozyrev et al., 2002; Spiridonov et al., 2011) and in other ore deposits of Russia (Cabri et al., 1975; Barkov et al., 2002; Tolstykh, 2008). Some analyses of the investigated majakite deviate from the ideal formula on the Ni(+Co) − As − Pd diagram, similar previous descriptions by (Distler et al., 1999; Sluzhenikin et al., 1994) (Fig. 11b). The fine intergrowths of these two minerals is quite possible, but it has been shown that there are limited solid solutions (with an immiscibility gap) between majakite and menshikovite ($Pd_3Ni_2As_3$) (Barkov et al., 2002). Our nonstoichiometric compositions of majakite seem to be similar to these solid solutions. The other minerals and unnamed phases in the samples in this study include various Pd-Ni arsenides with variable stoichiometry, which is less common.

Palladoarsenide (Pd_2As) contains Ni up to 14.65 wt%. The compositions show a slight enrichment in Pd (Table 7). The compositional plots are shifted to the Pd_5As_2 unnamed phase (Fig. 11b), indicating a solid solution between the two minerals. In contrast, Ni-rich palladoarsenide has been described as an exsolution texture with majakite (PdNiAs) (Evstigneeva and Trubkin, 2006; Spiridonov et al., 2011). The unnamed Pd_5As_2 was previously described in the Noril'sk 1 and Talnakh deposits (Mitenkov et al., 1997; Distler et al., 1999; Komarova et al.,

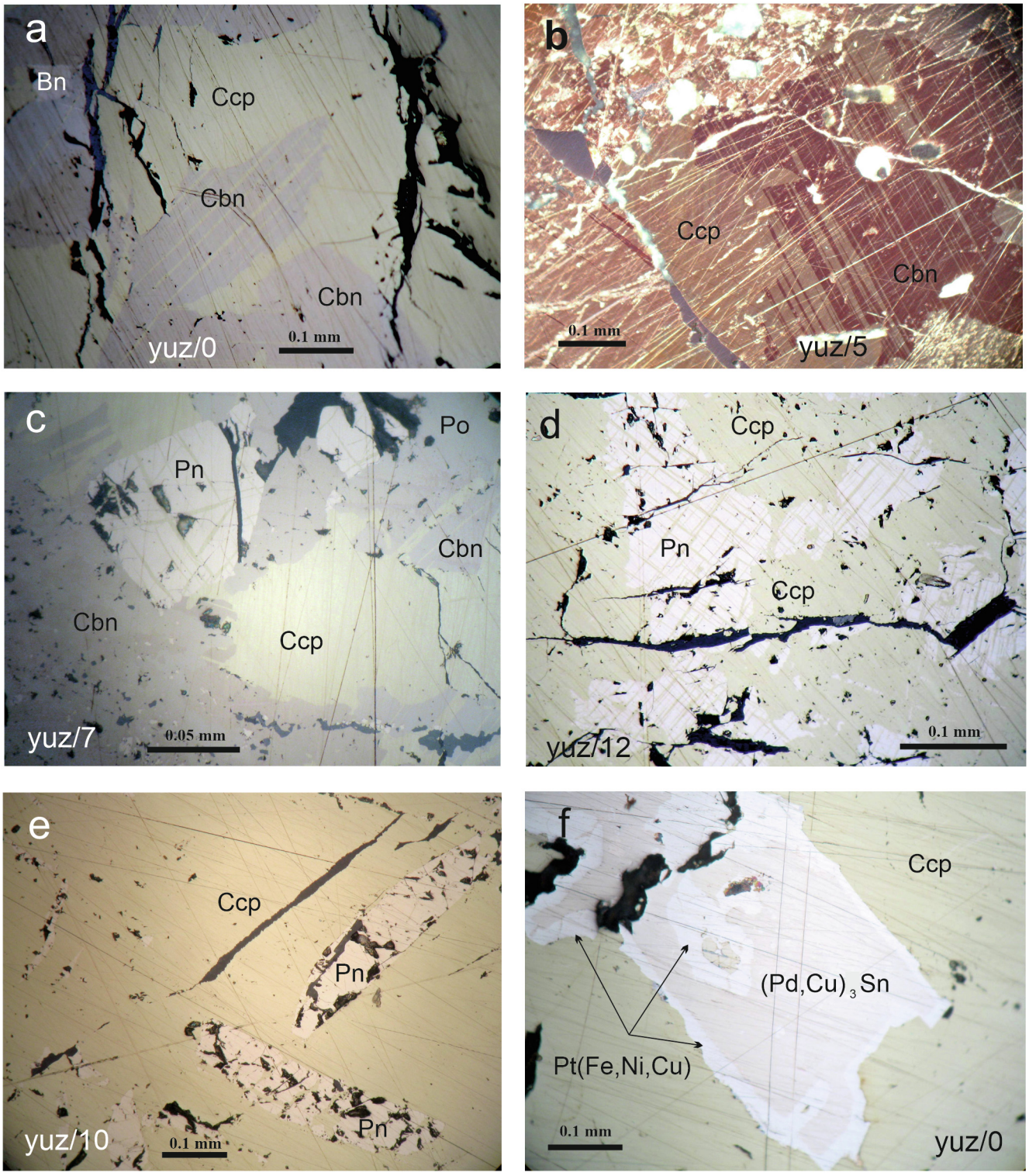

Fig. 7. Microphotographs in reflected light of sulphide minerals of the massive ore of the Southern-2 orebody: a, b – cubanite (Cbn) – chalcopyrite (Cpp) decomposition of solid solution (b – in crossed nicoles); c,d – pyrrhotite (Po)-cubanite-pentlandite (Pn)-chalcopyrite aggregate; e – lenticular pentlandite in chalcopyrite; f – crystal of stannopalladinite $(Pd,Cu)_3Sn$ which is banded by tetraferroplatinum Pt(Fe,Ni,Cu).

2002), whereas their Ni-rich analogue $(Ni,Pd)_5As_2$, or more precisely $Ni_7Pd_3As_4$, is a feature of the studied assemblage. The Southern-2 stillwaterite $(Pd,Ni)_8As_3$ and its Ni-rich analogue $(Ni,Pd)_8As_3$ occur as subhedral to euhedral crystals in polarite (Fig. 10i), whereas stillwaterite from other Noril'sk ores is Ni-poor (Kozyrev et al., 2002).

Unnamed phase Pd_3As contains no nickel, although it can accommodate up to 9 wt% Ni at temperatures higher than 450 °C (Gervilla et al., 1994). Minerals with compositions close to Pd_3As have been called various names, e.g. (1) an unnamed phase (Yu et al., 1974; Sluzhenikin et al., 1994; Komarova et al., 2002), (2) arsenopalladinite (Genkin et al., 1969; Kovalenker et al., 1972), (3) guanglinite (Distler et al., 1999; Sluzhenikin and Mokhov, 2008; Komarova et al., 2002), or (4) isomertieite (www.catalogmineralov.ru). The minor elements Sb and Sn, which can substitute arsenic, are typical of the mineral with a

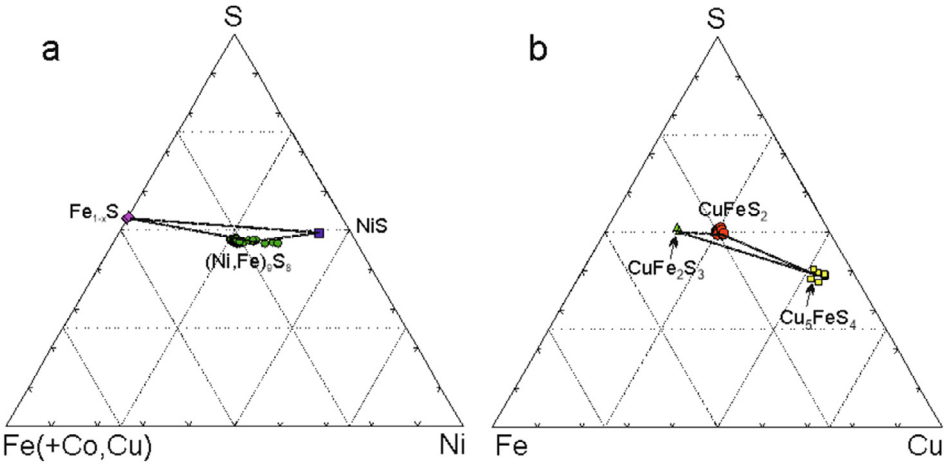

Fig. 8. Compositions of the Fe-Ni (a) and Fe-Cu sulphides (b) from massive ore of the Southern-2 orebody.

composition Pd_3As (Distler et al., 1999; Komarova et al., 2002).

5.2.3. Minerals of the Pd-Pb-Bi system

Zvyagintsevite, plumbopalladinite, polarite and unnamed Pd_5Pb_3 are the minerals of the Pd-Pb-Bi system and are present in the Southern-2 samples. These minerals occur as intergrowths with each other, ex-solutions of zvyagintsevite and galenite (Fig. 10j), as well as polarite, zvyagintsevite and Pd_5Pb_3 phase (Fig. 10k). Similar relationships among these minerals have been discussed previously (Genkin and Evstigneeva, 1986; Evstigneeva and Trubkin, 2010). The minerals of this system also often occur as intergrowths with Pd-rich tetra-auricupride.

Polarite Pd(Pb,Bi) is the most common Pd-Pb-Bi mineral occurring as symplectic intergrowths with zvyagintsevite. A solid solution of polarite was recorded in the compositions of the Pd-Pb-Bi minerals gradually ranging from $Pd(Pb_{0.85}Bi_{0.15})$ to $Pd_{1.01}(Bi_{0.59}Pb_{0.40})_{0.99}$. Bi dominates in the four analyses, one of which shows the greatest enrichment of bismuth (up to 78 at.%) (Table 6, Fig. 12). In general, the compositions of polarite range from almost pure PdBi to Pd $(Pb_{0.80}Bi_{0.20})$ (Genkin et al., 1969; Evstigneeva and Genkin, 1990; Kozyrev et al., 2002; Spiridonov et al., 2003; Sluzhenikin and Mokhov, 2007). Bismuth-rich species of polarite are typical of Noril'sk 1 ores,

Table 4
Composition of sulphides from Southern-2 orebody of the Talnakh intrusion (wt. %).

No	Sample	Fe	Cu	Ni	Co	S	Total	Formula:
1	yuz/0	61.26		0.05		39.18	100.51	$Fe_{0.95}S_{1.05}$
2	yuz/0	60.92		0.10		39.37	100.45	$Fe_{0.94}S_{1.06}$
3	yuz/0	59.85		0.09		39.65	99.63	$Fe_{0.93}S_{1.07}$
4	yuz/0	1.81	5.82	55.58	1.59	34.13	98.93	$(Ni_{0.88}Cu_{0.08}Fe_{0.03}Co_{0.02})_{1.01}S_{0.98}$
5	yuz/5	31.68	0.06	34.13	0.45	33.51	99.83	$(Ni_{4.49}Fe_{4.38}Co_{0.06}Cu_{0.01})_{8.94}S_{8.07}$
6	yuz/5	31.00	0.06	34.19	0.53	32.48	98.26	$(Ni_{4.58}Fe_{4.37}Co_{0.07}Cu_{0.01})_{9.03}S_{7.97}$
7	yuz/10	31.23		34.69	0.47	33.06	99.44	$(Ni_{4.59}Fe_{4.34}Co_{0.06})_{8.99}S_{8.00}$
8	yuz/10	31.61	0.06	34.70	0.54	33.25	100.16	$(Ni_{4.56}Fe_{4.37}Co_{0.07}Cu_{0.01})_{9.01}S_{8.00}$
9	yuz/12	30.81		34.85	0.52	33.01	99.19	$(Ni_{4.62}Fe_{4.29}Co_{0.07})_{8.98}S_{8.01}$
10	yuz/12	31.40	0.06	35.24	0.48	32.86	100.04	$(Ni_{4.65}Fe_{4.35}Co_{0.06}Cu_{0.01})_{9.07}S_{7.93}$
11	yuz/11	30.60	0.06	35.48	0.46	33.06	99.65	$(Ni_{4.69}Fe_{4.25}Co_{0.06}Cu_{0.01})_{9.01}S_{8.00}$
12	yuz/11	29.88		36.46	0.45	33.14	99.93	$(Ni_{4.80}Fe_{4.14}Co_{0.06})_{9.00}S_{7.99}$
13	yuz/11	29.52	0.08	36.69	0.53	33.04	99.86	$(Ni_{4.84}Fe_{4.09}Co_{0.07}Cu_{0.01})_{9.01}S_{7.98}$
14	yuz/0	27.96	0.09	37.63	0.41	33.24	99.33	$(Ni_{4.98}Fe_{3.89}Co_{0.05}Cu_{0.01})_{8.93}S_{8.06}$
15	yuz/0	27.74	0.20	37.85	0.41	33.29	99.49	$(Ni_{5.01}Fe_{3.86}Co_{0.05}Cu_{0.02})_{8.94}S_{8.06}$
16	yuz/12	26.60	0.20	38.98	0.42	33.06	99.26	$(Ni_{5.17}Fe_{3.71}Co_{0.06}Cu_{0.02})_{8.96}S_{8.03}$
17	yuz/0	26.47	0.13	39.25	0.44	33.19	99.48	$(Ni_{5.20}Fe_{3.68}Co_{0.06}Cu_{0.02})_{8.96}S_{8.05}$
18	yuz/0	26.10	0.12	39.82	0.39	33.27	99.70	$(Ni_{5.26}Fe_{3.62}Co_{0.05}Cu_{0.01})_{8.94}S_{8.05}$
19	yuz/12	23.73	0.13	42.55	0.42	32.63	99.46	$(Ni_{5.66}Fe_{3.32}Co_{0.06}Cu_{0.02})_{9.06}S_{7.95}$
20	yuz/12	21.46	0.26	44.64	0.47	32.80	99.63	$(Ni_{5.93}Fe_{3.00}Co_{0.06}Cu_{0.03})_{9.02}S_{7.98}$
21	yuz/12	20.28	0.35	46.29	0.48	32.82	100.21	$(Ni_{6.12}Fe_{2.82}Co_{0.06}Cu_{0.04})_{9.04}S_{7.95}$
22	yuz/7	30.28	34.28			35.14	99.70	$Cu_{0.99}Fe_{1.00}S_{2.01}$
23	yuz/11	30.23	34.63			34.95	99.81	$Cu_{1.00}Fe_{0.99}S_{2.00}$
24	yuz/11	30.31	34.63			34.47	99.42	$Cu_{1.01}Fe_{1.00}S_{1.99}$
25	yuz/12	30.49	34.75			34.07	99.31	$Cu_{1.01}Fe_{1.01}S_{1.97}$
26	yuz/0	40.60	22.65			35.17	98.42	$Fe_{2.00}Cu_{0.98}S_{3.02}$
27	yuz/7	40.72	21.70			36.04	98.46	$Fe_{1.99}Cu_{0.93}S_{3.07}$
28	yuz/7	40.45	22.82	0.11		35.35	98.73	$Fe_{1.99}Cu_{0.98}Ni_{0.01}S_{3.02}$
29	yuz/0	9.44	65.78			23.01	98.23	$Cu_{5.39}Fe_{0.88}S_{3.73}$
30	yuz/0	7.46	68.07	0.15		24.52	100.19	$Cu_{5.43}(Fe_{0.68}Ni_{0.01})_{0.69}S_{3.88}$
31	yuz/0	8.79	66.50	0.05		25.17	100.51	$Cu_{5.26}Fe_{0.79}S_{3.95}$
32	yuz/0	8.63	66.02			25.32	99.97	$Cu_{5.24}Fe_{0.78}S_{3.98}$
33	yuz/0	9.19	64.90	0.06		25.80	99.95	$Cu_{5.13}(Fe_{0.83}Ni_{0.01})_{0.84}S_{4.04}$

Note: 1–3 – pyrrhotite FeS, 4 – millerite NiS, 5–21 – pentlandite $(Fe,Ni)_9S_8$, 22–25 – chalcopyrite $CuFeS_2$, 26–28 – cubanite $CuFe_2S_3$; 29–33 – bornite Cu_5FeS_4. The empty cell – concentration of element is below detection limit (here and below).

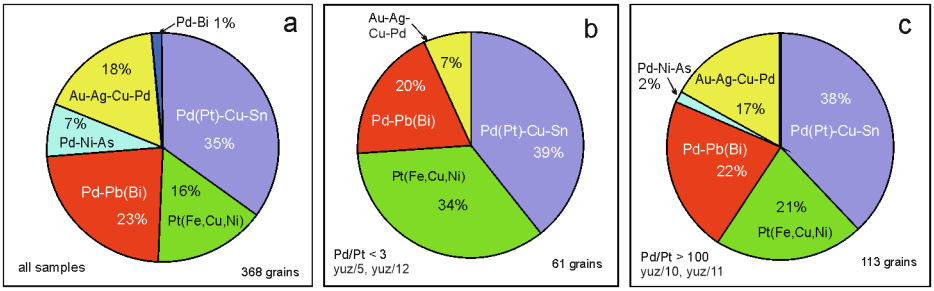

Fig. 9. Ratios of PGMs and gold grains in all six studied samples of Southern-2 orebody (a), in samples with Pd/Pt values < 3 (b) and Pd/Pt values > 100 (c).

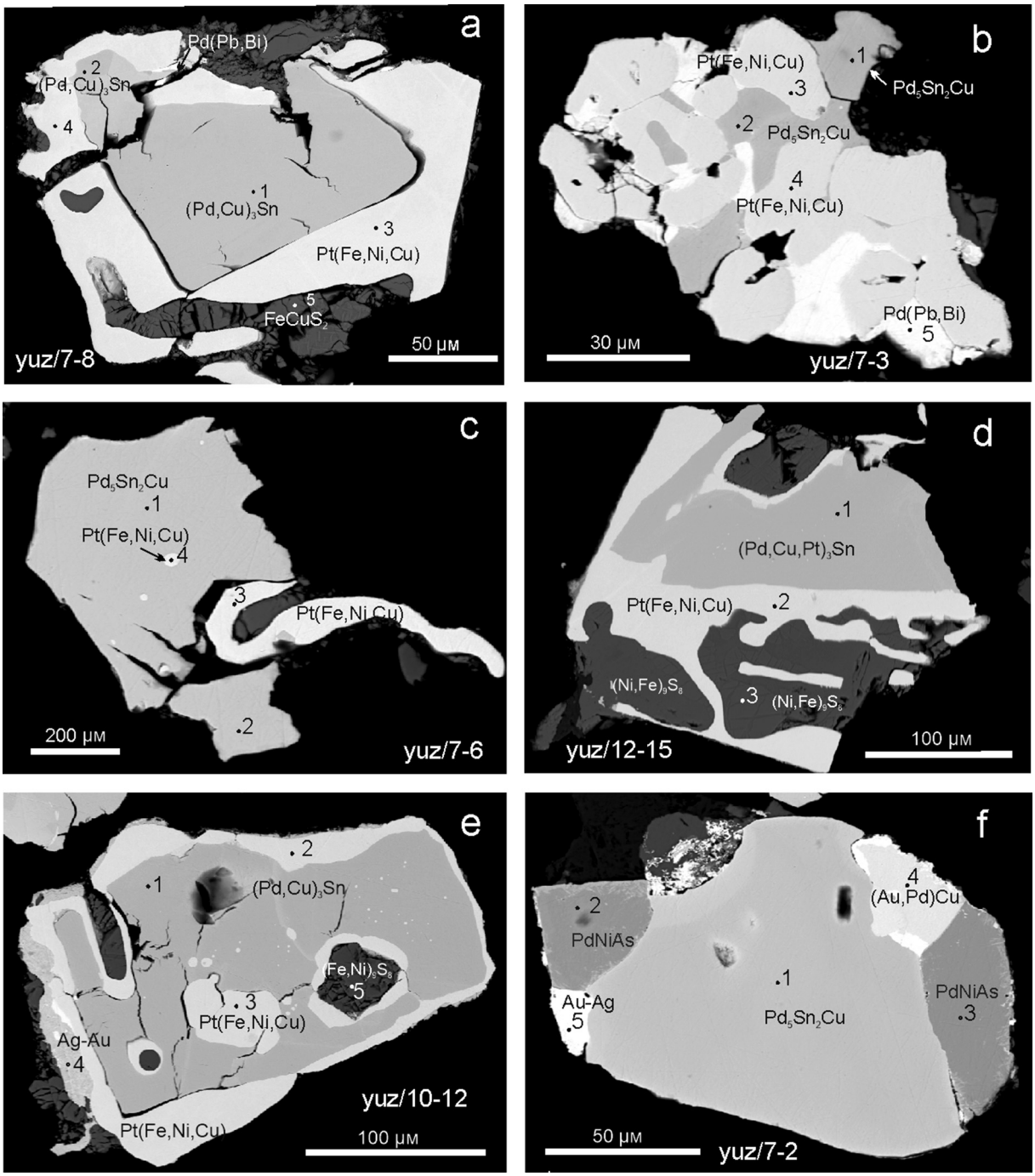

Fig. 10. Backscattered electrons (BSE) images: microparageneses of PGE minerals from the south-western branch of the Talnakh intrusion. EDS analyses in points are shown in Table 6.

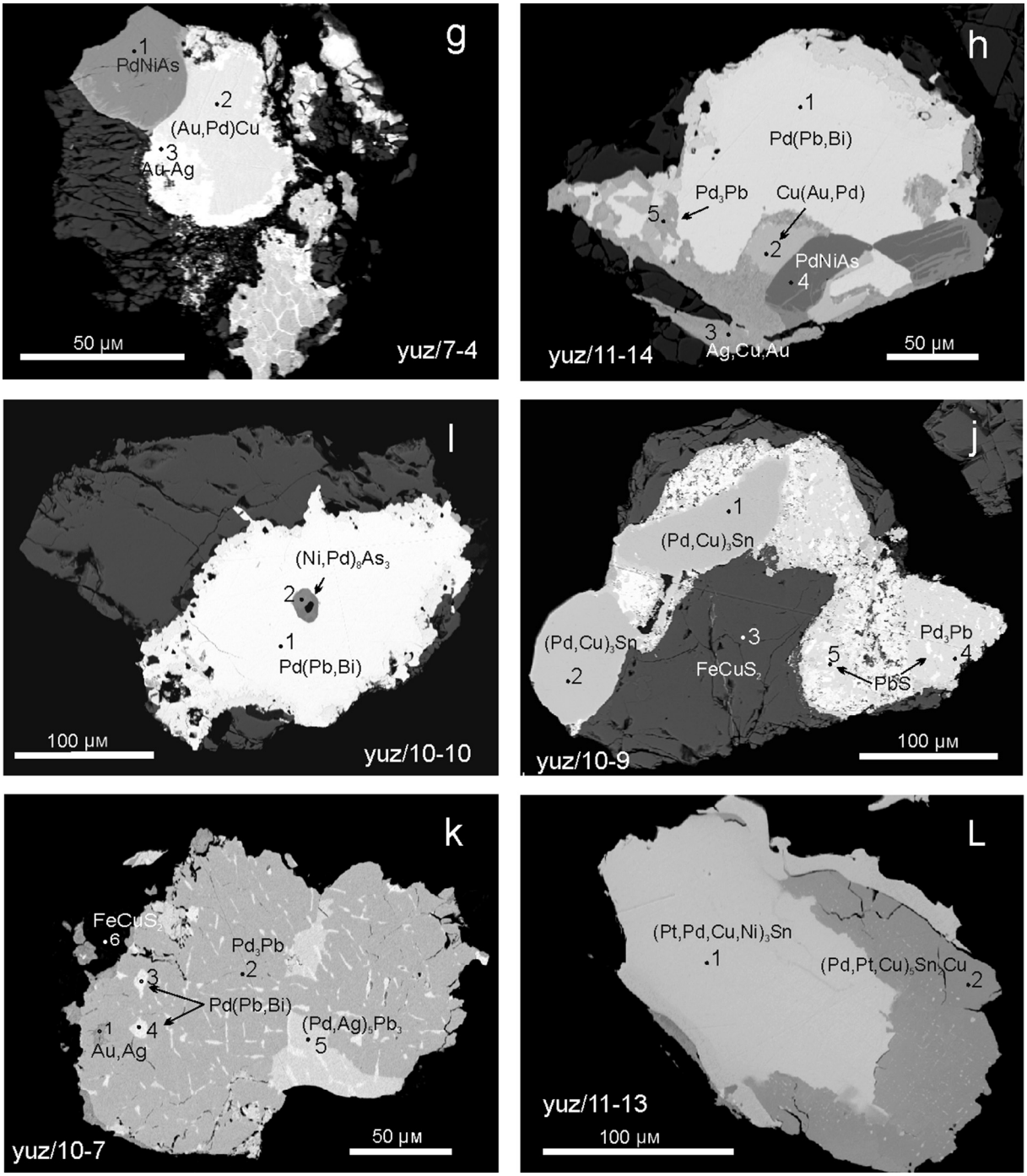

Fig. 10. (*continued*)

whereas Pb-rich species are typical of Talnakh (Fig. 12). It is noteworthy that the highest concentration of Pb in polarite exceeding 80 mol.% has not previously been reported.

Zvyagintsevite (Pd_3Pb) occurs as intergrowths with other Pb-minerals, including with galena, to form a spotted texture (Fig. 10j, k). The composition of this mineral corresponds to the stoichiometry (Table 8, Fig. 12). Plumbopalladinite (Pd_3Pb_2) contains Bi up to 9.22 wt % and minor Pt and Sn (Table 8, Fig. 12) and is similar to that previously described in the Noril'sk 1 deposit (Spiridonov et al., 2003). Detailed studies of Pd-Pb-Bi minerals have shown that frequent deviation of plumbopalladinite composition from its stoichiometry can be attributed to the presence of micron-sized inclusions of other Pd_2Pb phase (Evstigneeva and Trubkin, 2009, 2010). The unnamed mineral corresponding to Pd_5Pb_3 occurs intergrown with other Pb-minerals (Fig. 10k), tetra-auricupride and Ag-Au alloys, and reaches grain sizes of up to 100 μm. The compositions of this phase correspond to stoichiometry 5/3 (Fig. 12). It was classified as an unnamed phase (Krivolutskaya et al., 2018), but in composition it is close to the recently described noril'skite mineral $(Pd,Ag)_7Pb_4$ (Vymazalova et al., 2017), since the studied phase consistently includes Ag (0.77–3.09 wt %), similar to noril'skite. The composition of the studied phase corresponds more to stoichiometry Pd_5Pb_3, similar to a synthetic phase, which is stable over a wide range of temperatures (Mamontov, 1999).

5.2.4. *Minerals of the Pd-Pt-Cu-Sn system*

Minerals of the Pd-Pt-Cu-Sn system have been discovered in the

Table 5
Compositions of Pt-Fe-Ni-Cu alloys (wt. %).

No	Sample	Pt	Pd	Ni	Cu	Fe	Rh	Total	Formula:
1	yuz/11	76.48	0.63	3.53	2.97	16.14	0.12	99.87	$Pt_{0.99}(Fe_{0.73}Ni_{0.15}Cu_{0.12}Pd_{0.01})_{1.01}$
2	yuz/12	76.08	0.28	3.63	2.66	16.45	0.26	99.36	$Pt_{0.98}(Fe_{0.74}Ni_{0.16}Cu_{0.11}Pd_{0.01}Rh_{0.01})_{1.02}$
3	yuz/12	76.67	0.72	3.60	2.98	15.36	0.05	99.38	$Pt_{1.00}(Fe_{0.70}Ni_{0.16}Cu_{0.12}Pd_{0.02})_{1.00}$
4	yuz/11	76.91	0.34	3.65	2.53	16.33		99.76	$Pt_{1.00}(Fe_{0.74}Ni_{0.16}Cu_{0.10}Pd_{0.01})_{1.00}$
5	yuz/11	76.67	0.23	3.65	2.53	16.22		99.3	$Pt_{1.00}(Fe_{0.73}N_{0.16}Cu_{0.10}Pd_{0.01})_{1.00}$
6	yuz/12	76.33	0.27	3.69	2.65	15.99	0.10	99.03	$Pt_{1.00}(Fe_{0.72}Ni_{0.16}Cu_{0.11}Pd_{0.01})_{1.00}$
7	yuz/12	76.27	0.17	3.77	2.55	16.33	0.13	99.22	$Pt_{0.99}(Fe_{0.74}Ni_{0.17}Cu_{0.10})_{1.01}$
8	yuz/10	76.21	0.40	3.77	2.45	15.75	0.10	98.68	$Pt_{1.00}(Fe_{0.73}Ni_{0.16}Cu_{0.10}Pd_{0.01})_{1.00}$
9	yuz/11	75.20	1.22	3.85	2.51	15.23	0.05	98.06	$Pt_{0.99}(Fe_{0.71}Ni_{0.17}Cu_{0.10}Pd_{0.03})_{1.01}$
10	yuz/12	76.57	0.37	4.07	2.53	15.72	0.09	99.35	

Note: WDS data.

massive Cu-rich ores of the Southern-2 orebody (Fig. 10a–f, l). Sporadic grains of rustenburgite are banded by stannopalladinite (Fig. 10l). Rustenburgite-atokite compositions include Cu (up to 2.06 wt%) and Ni (up to 1.75 wt%) (Table 9, Fig. 13) and corresponds to $(Pt,Pd,Cu,Ni)_3Sn$ formula, similar to that shown by Genkin and Evstigneeva (1986).

Stannopalladinite (Pd_5Sn_2Cu) occurs in almost in all samples in the present study as intergrowths with Pd_3Pb, PdNiAs, tetraferroplatinum and Au-Pd-Cu alloys (Fig. 10). In contrast, this mineral was not reported in all types of massive ores of the Oktyabr'sky deposit (Kozyrev et al., 2002; Komarova et al., 2002) and was described only at the Noril'sk 1 deposit (Spiridonov et al., 2003; Tolstykh and Podlipsky, 2010). Stannopalladinite in this study contains Pt up to 19.94 wt% and Pb up to 5.94 wt% (Table 9), which should correspond to formula $(Pd,Pt)_5(Sn,Pb)_2Cu$.

The composition of stannopalladinite deviates from the stoichiometric formula, because the amount of copper in most analyses exceeds the required amount of Cu for one formula unit: $(Pd,Pt)_{5-x}(Sn,Pb)_2Cu_{1+x}$ (Fig. 13a). The Southern-2 stannopalladinite is also compositionally different from those of the Noril'sk 1 intrusion (Spiridonov et al., 2003), which on the contrary lacks copper.

All compositions of stannopalladinite from this study plot between stoichiometric stannopalladinite and taimyrite (closer to the former) in the Sn + Pb − Pd + Pt − Cu(+Ni) diagram (Fig. 13a). Copper in the crystal structure of stannopalladinite should occupy its own position to give the formula of Pd_5Sn_2Cu. The surplus above of one formula unit of Cu will substitute for platinum in the structure (but not palladium) since there is a positive correlation of copper excess (Cu*) with palladium (Fig. 14a) and negative correlation of Cu* with platinum (Fig. 14b) observed. In this case, the recalculated compositions of stannopalladinite show a relatively narrow trend in the diagram (Fig. 13b) and correspond to the formula $(Pd,Pt,Cu^*)_5(Sn,Pb)_2Cu$ where Cu* is excess of Cu above one formula unit.

5.2.5. *Minerals of the Au-Ag-Pd-Cu system*

Intermetallics of the Au-Ag-Pd-Cu system occur as intergrowths with PGMs (Fig. 10e–f). The assemblage of intermetallic minerals is dominated by tetra-auricupride Cu(Au,Pd) (Pd varies from 7 to 10 wt%) with subordinate amounts of auricupride $Cu_3(Au,Pd)$, and Au-Ag solid solutions in variable proportions (Table 10). The grains of tetra-auricupride are often surrounded by rims of Au-Ag alloys (Fig. 10g). All the Au-Ag-Pd-Cu intermetallics of the Southern-2 orebody have been also found in other Cu-Ni ores of the Noril'sk deposit (Sluzhenikin and Mokhov, 2015).

6. Discussion

6.1. *Geochemical variation in the ores*

The Southern-2 orebody is composed of predominately of chalcopyrite ores with minor increasing amounts of pyrrhotite in the lower part of the orebody. This study did observe any low-sulphur minerals (Distler et al., 1975) (mooihoekite, talnakhite, putoranite), which are characteristic of the central part of the Oktyabr'sky deposit (Distler et al., 1975; Kozyrev et al., 2002). The massive sulphide ores of the Southern-2 orebody are rich in copper and nickel (Cu up to 28.12 and 10.58 wt%, Ni up to 6.29 and 2.45 wt%) in massive and disseminated ores. The Ni/Cu ratio in massive ores is on average 0.19, similar to that of the disseminated and vein-disseminated ores in gabbro-dolerite, in which the Ni/Cu ratio is 0.21 on average. This ratio is slightly higher than the mooihoekite ores of the Oktyabr'sky deposit (Ni/Cu = 0.11). In contrast, the massive pyrrhotite ores of all intrusions are characterized by higher Ni/Cu (1.22–1.36) (Distler and Kunilov, 1994; Sluzhenikin et al., 2014).

The total of Pt + Pd in massive ore of Southern-2 is 103.5 ppm, and disseminated ores are also enriched in Pt + Pd (84.4 ppm). The Pd/Pt ratio is more than 1 in all samples, but varies from 2.14 to 8.74 for the

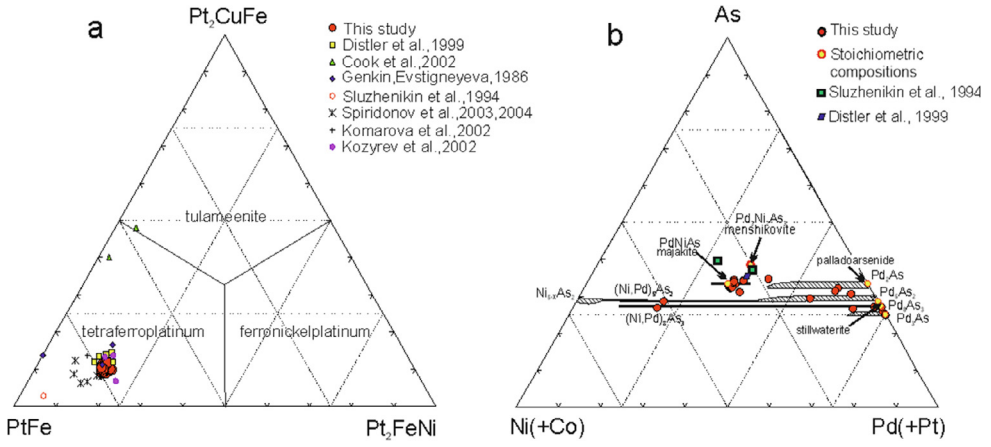

Fig. 11. Compositions of Pt-Fe-Ni-Cu alloys in the tetraferroplatinum – ferronickelplatinum – tulameenite systems compared to the compositions of these alloys in the Noril'sk-Talnakh ores from previous studies (a); compositions of PGE minerals in the Pd-Ni-As system (at.%) (b). Stability fields at 450 °C were taken from Gervilla et al. (1994).

Table 6
Compositions of minerals, shown in microphotographs (Fig. 10).

No. photo Fig. 10	Point	Fe	Ni	Cu	Au	Ag	Pt	Pd	Sn	Pb	Bi	As	S	Total	Formula
yuz/7–7	1			9.09			2.75	59.97	28.13					99.94	$(Pd_{4.70}Pt_{0.12}Cu_{0.20})_{5.02}Sn_{1.98}Cu_{1.00}$
yuz/7–7	2			9.22			1.90	60.32	27.62	1.72				100.788	$(Pd_{4.71}Pt_{0.08}Cu_{0.21})_{5.00}(Sn_{1.93}Pb_{0.07})_{2.00}Cu_{1.00}$
yuz/7–7	3	15.53	3.94	2.03			77.87							99.37	$Pt_{1.03}(Fe_{0.72}Ni_{0.17}Cu_{0.08})_{0.97}$
yuz/7–7	4	15.90	3.89	2.92			78.07							100.78	$Pt_{1.00}(Fe_{0.71}Ni_{0.17}Cu_{0.12})_{2.00}$
yuz/7–7	5	29.31		33.85		0.64								98.53	$Ni_{5.64}Fe_{3.29}S_{8.06}$
yuz/7–3	1			9.79			5.12	58.1	27.21					100.22	$(Pd_{4.57}Cu_{0.29}Pt_{0.22})_{5.08}Sn_{1.92}Cu_{1.00}$
yuz/7–3	2			8.12			3.98	59.92	27.5					99.52	$(Pd_{4.78}Pt_{0.17}Cu_{0.08})_{5.03}Sn_{1.97}Cu_{1.00}$
yuz/7–3	3	16.09	4.12	2.9			77.22							100.33	$Pt_{0.99}(Fe_{0.72}Ni_{0.18}Cu_{0.11})_{1.01}$
yuz/7–3	4	15.15	4.22	2.77			77.50							99.64	$Pt_{1.01}(Fe_{0.69}Ni_{0.19}Cu_{0.11})_{0.99}$
yuz/7–3	5							34.91		48.12	17.33			100.36	$Pd_{1.02}(Pb_{0.72}Bi_{0.26})_{0.98}$
yuz/7–6	1			9.13			4.52	57.14	23.43	5.44				99.66	$(Pd_{4.63}Cu_{0.24}Pt_{0.20})_{5.07}(Sn_{1.70}Pb_{0.23})_{1.93}Cu_{1.00}$
yuz/7–6	2			9.43			4.38	57.84	23.43	5.56				100.64	$(Pd_{4.63}Cu_{0.26}Pt_{0.19})_{5.09}(Sn_{1.68}Pb_{0.23})_{1.91}Cu_{1.00}$
yuz/7–6	3	15.09	4.10	3.75			78.30							101.26	$Pt_{0.98}(Fe_{0.70}Ni_{0.17}Cu_{0.14})_{1.01}$
yuz/7–6	4	16.71	3.70	2.83			77.40							100.64	$Pt_{0.99}(Fe_{0.74}Ni_{0.16}Cu_{0.11})_{1.01}$
yuz/12–15	1			8.82			4.51	57.08	26.76					97.17	$(Pd_{4.65}Cu_{0.20}Pt_{0.20})_{5.05}Sn_{1.95}Cu_{1.00}$
yuz/12–15	2	16.33	4.19	2.72			74.38							97.62	$Pt_{0.97}(Fe_{0.74}Ni_{0.18}Cu_{0.11})_{1.03}$
yuz/12–15	3	22.16	44.8										33.34	100.3	$(Ni_{5.90}Fe_{3.07})_{8.96}S_{8.03}$
yuz/10–12	1			9.91			4.82	55.79	27.91					98.43	$(Pd_{4.46}Cu_{0.33}Pt_{0.21})_{5.00}Sn_{2.00}Cu_{1.00}$
yuz/10–12	2	16.15	3.43	2.88			75.18							97.64	$Pt_{0.99}(Fe_{0.74}Ni_{0.15}Cu_{0.12})_{1.01}$
yuz/10–12	3	16.98	3.95	2.91			76.26							100.10	$Pt_{0.97}(Fe_{0.75}Ni_{0.17}Cu_{0.11})_{1.03}$
yuz/10–12	4			1.07	28.65	68.48								98.20	$Ag_{0.80}Au_{0.18}Cu_{0.02}$
yuz/10–12	5	28.35	37.12										32.66	98.13	$(Ni_{4.98}Fe_{4.00})_{8.98}S_{8.02}$
yuz/7–2	1			9.98			3.54	57.45	27.92					98.89	$(Pd_{4.54Pt0.15}Cu_{0.44})_{5.14}Sn_{1.98}Cu_{1.00}$
yuz/7–2	2		24.32					44.23				31.12		99.67	$Pd_{1.00}Ni_{1.00}As_{1.00}$
yuz/7–2	3		24.20					44.61				31.40		100.21	$Pd_{1.01}Ni_{0.99}As_{1.00}$
yuz/7–2	4			26.35	66.5			7.21						100.06	$Cu_{1.01}(Au_{0.82}Pd_{0.17})_{0.99}$
yuz/7–2	5				74.35	26.18								100.53	$Au_{0.61}Ag_{0.39}$
yuz/7–4	1		24.18					44.49				31.80		100.47	$Pd_{1.00}Ni_{0.99}As_{1.02}$
yuz/7–4	2			26.08	65.01			7.69						98.78	$Cu_{1.01}(Au_{0.81}Pd_{0.18})_{0.99}$
yuz/7–4	3			1.98	68.95	26.32								97.25	$Au_{0.56}Ag_{0.39}Cu_{0.05}$
yuz/11–14	1							33.88		36.19	27.12			97.19	$Pd_{1.02}(Pb_{0.56}Bi_{0.42})_{0.98}$
yuz/11–14	2			26.71	63.18			8.50						98.39	$Cu_{1.02}(Au_{0.78}Pd_{0.19})_{0.97}$
yuz/11–14	3			20.13	32.82	46.19								99.14	$Ag_{0.47}Cu_{0.35}Au_{0.18}$
yuz/11–14	4		23.93					43.91				30.86		98.7	$Pd_{1.00}Ni_{0.99}As_{1.00}$
yuz/11–14	5							59.60		38.74				98.34	$Pd_{3.00}Pb_{1.00}$
yuz/10–10	1							33.89		28.35	36.30			98.54	$Pd_{1.01}(Bi_{0.55}Pb_{0.44})_{0.99}$
yuz/10–10	2		42.78					28.98				27.56		99.32	$(Ni_{5.86}Pd_{2.19})_{8.05}As_{2.96}$
yuz/10–9	1			7.62			1.12	62.17	21.41	1.02		5.82		99.16*	$(Pd_{4.96}Pt_{0.05}Cu_{0.02})_{5.03}(Sn_{1.53}Sb_{0.41}Pb_{0.04})_{1.98}Cu_{1.00}$
yuz/10–9	2			7.39			1.18	62.01	21.08	1.49		5.64		98.79*	$(Pd_{4.98}Pt_{0.05})_{5.03}(Sn_{1.52}Sb_{0.40}Pb_{0.06})_{1.98}Cu_{0.98}$
yuz/10–9	3	29.96		33.85									35.09	98.90	$Cu_{0.98}Fe_{0.99}S_{2.02}$
yuz/10–9	4							61.57		38.18				99.75	$Pd_{3.03}Pb_{0.97}$
yuz/10–9	5									84.62			13.66	98.28	$Pb_{0.98}S_{1.02}$
yuz/10–7	1				30.55	68.28								98.83	$Ag_{0.80}Au_{0.20}$
yuz/10–7	2							61.88		39.59				101.47	$Pd_{3.01}Pb_{0.99}$
yuz/10–7	3							35.15		37.78	27.64			100.57	$Pd_{1.02}(Pb_{0.57}Bi_{0.41})_{0.98}$
yuz/10–7	4							34.42		56.31	9.32			100.05	$Pd_{1.01}(Pb_{0.85}Bi_{0.14})_{0.99}$
yuz/10–7	5					3.18		43.40		52.88				99.46	$(Pd_{4.71}Ag_{0.34})_{5.05}Pb_{2.95}$
yuz/10–7	6	30.25		33.82									35.67	99.74	$Cu_{0.97}Fe_{0.99}S_{2.04}$
yuz/11–13	1		1.85	2.25			61.19	13.29	20.12					98.70	$(Pt_{1.86}Pd_{0.74}Cu_{0.21}Ni_{0.19})_{3.00}Sn_{1.00}$
yuz/11–13	2			8.89			28.44	35.77	24.38					97.48	$(Pd_{3.25}Cu_{0.35}Pt_{1.41})_{5.01}Sn_{1.99}Cu_{1.00}$

Note: Analyses carried by EDS (see. Methods of Research). * – the totals include 0.41 and 0.40 wt% Sb.

most grains (Table 3). The similar Pd/Pt ratio is also characteristic for disseminated and vein-disseminated ores (1.24–6.61). The chondrite-normalized patterns of PGEs and other metals (Fig. 4) show that the PPGE/IPGE ratios reach 44.98 (Table 3), and the Rh vs. Cu diagram (Fig. 15) shows significant fractionation of PGEs (more than 80%) in ores in this study, which are more fractionated than others in the Noril'sk region (Naldrett, 2004) (Fig. 15). The PPGE/IPGE in the studied samples is three orders higher than that of the pyrrhotite ores (1–20) and one order higher (285–470) than the talnakhite and mooihoekite ores (Dodin et al., 2009). PGE minerals from the Southern-2 orebody crystallized from a residual and much fractionated sulphide melt, which was significantly more enriched in Cu, Ni, Pt and Pd and depleted in refractory PGEs.

Table 3 shows relationships between PGEs and sulphur (PGE/S), Cu and Pd (Cu/Pd), Ni and Ir (Ni/Ir) and other elements, which can be used to characterize of the Souther-2 ores. The Cu/Pd ratio in primary mantle magmas is approximately 6500 (Barnes et al., 1988). Rocks in which the Cu/Pd ratios are below this value contain Pd-rich sulphides as a rule, whereas rocks with Cu/Pd ratios above 6500 may have crystallized from magma that has lost Pd as a result of a sulphide segregation process (Maier et al., 1998, 2008). The Cu/Pd ratios in the Southern-2 ores are 3230 on average in massive, and 2240 in disseminated ores (Table 3). Similar values are given in Duran et al. (2017): 800–2100 for Noril'sk ores of various types and 3500–6000 for Talnakh ores.

The concentration of metals is positively correlates with the content of sulphur in rocks containing disseminated sulphide, which was caused by a single process of the sulphur segregation (Helmy, 2004; Maier et al., 2008) and enrichment of the sulphide liquid in Cu, PGEs and Au, due to the very high partition coefficients between the sulphide and

Table 7
Composition of PGE minerals in the Pd-Ni-As system (wt.%).

No		Fe	Co	As	Pd	Ni	Total	Formula:
1	Yuz/7	0.15	0.13	30.7	46.96	20.12	98.06	$Pd_{1.10}(Ni_{0.86}Fe_{0.01}Co_{0.01})_{0.88}As_{1.02}$
2	Yuz/7	0.4	0.06	31.59	44.83	21.71	98.59	$Pd_{1.03}(Ni_{0.91}Fe_{0.03})_{0.94}As_{1.03}$
4	Yuz/7			31.08	45.32	22.81	99.21	$Pd_{1.04}Ni_{0.95}As_{1.01}$
5	Yuz/7		0.09	30.08	45.44	22.95	98.56	$Pd_{1.05}Ni_{0.96}As_{0.99}$
6	Yuz/7	0.07	0.17	29.72	45.68	23.32	98.96	$Pd_{1.05}(Ni_{0.97}Co_{0.01})_{0.98}As_{0.97}$
7	Yuz/7		0.13	29.59	45.1	23.15	97.97	$Pd_{1.05}(Ni_{0.97}Co_{0.01})_{0.98}As_{0.97}$
8	Yuz/7	0.09	0.13	29.85	45.18	23.31	98.56	$Pd_{1.04}(Ni_{0.97}Co_{0.01})_{0.98}As_{0.98}$
9	Yuz/7		0.19	29.71	45.61	23.37	98.88	$Pd_{1.05}(Ni_{0.97}Co_{0.01})_{0.98}As_{0.97}$
10	Yuz/7	0.1	0.12	29.93	45.38	23.54	99.07	$Pd_{1.04}(Ni_{0.98}Co_{0.01})_{0.99}As_{0.98}$
11	Yuz/7		0.06	29.86	45.01	23.39	98.32	$Pd_{1.04}Ni_{0.98}As_{0.98}$
12	Yuz/7	0.12	0.13	29.57	44.92	23.52	98.26	$Pd_{1.04}(Ni_{0.98}Fe_{0.01}Co_{0.01})_{1.00}As_{0.97}$
13	Yuz/7	0.05	0.11	29.63	45.22	23.67	98.68	$Pd_{1.04}Ni_{0.99}As_{0.97}$
14	Yuz/7		0.13	29.69	45.22	23.71	98.75	$Pd_{1.04}(Ni_{0.99}Co_{0.01})_{1.00}As_{0.97}$
15	Yuz/7	0.06	0.09	29.97	44.04	23.63	97.79	$Pd_{1.02}Ni_{0.99}As_{0.98}$
16	Yuz/7		0.08	23.97	71.36	3.22	98.63	$(Pd_{1.92}Ni_{0.16})_{2.08}As_{0.92}$
17	Yuz/7		0.17	25.01	67.88	5.04	98.1	$(Pd_{1.80}Ni_{0.24}Co_{0.02})_{2.06}As_{0.94}$
18	Yuz/7	0.07	0.14	25.55	68.12	4.57	98.45	$(Pd_{1.81}Ni_{0.22}Co_{0.01})_{2.04}As_{0.96}$
19	Yuz/7	0.54	0.11	30.37	52.73	14.65	98.4	$(Pd_{1.27}Ni_{0.65}Fe_{0.02})_{1.94}As_{1.06}$
20	Yuz/7		0.1	20.85	77.83		98.77	$(Pd_{7.95}Co_{0.02}Fe_{0.01})_{7.98}As_{3.02}$
21	Yuz/10			20.96	80.48		101.44	$Pd_{8.03}As_{2.97}$
22	Yuz/7	0.11		20.78	77.33	0.8	99.02	$(Pd_{7.83}Ni_{0.15}Fe_{0.02}Co_{0.01})_{8.01}As_{2.99}$
23	Yuz/7	0.08		21.05	74.96	4.13	100.22	$(Pd_{7.33}Ni_{0.73}Fe_{0.01}Co_{0.01})_{8.08}As_{2.92}$
24	Yuz/7			18.83	80.37	0.05	99.25	$(Pd_{2.99}Ni_{0.01})_{3.00}As_{1.00}$
25	Yuz/7			18.89	80.5		99.39	$Pd_{3.00}As_{1.00}$
26	Yuz/7	0.14		19.32	78.46		97.92	$(Pd_{2.95}Fe_{0.01})_{2.96}As_{1.04}$
27	Yuz/7		0.1	19.4	78.78	0.05	98.33	$(Pd_{2.96}Co_{0.01})_{2.97}As_{1.03}$
28	Yuz/7			27.56	28.98	42.78	99.32	$(Ni_{5.86}Pd_{2.19})_{8.05}As_{2.96}$ or $Ni_{7.98}Pd_{2.99}As_{4.03}$
29	Yuz/7	0.09	0.14	24.36	64.96	10.01	99.56	$(Pd_{3.85}Ni_{1.08}Fe_{0.01}Co_{0.01})_{4.95}As_{2.05}$
30	Yuz/10			28.44	29.29	39.33	97.26*	$(Ni_{3.54}Pd_{1.46}Pt_{0.01})_{5.01}As_{2.00}$

Note: 1–15 – majakite PdNiAs; 16–19 – palladoarsenide Pd_2As; 20–23 – stillwaterite Pd_8As_3; 24–27 – unnamed phase Pd_3As; 28 – Ni-rich analogue of stillwaterite $(Ni,Pd)_8As_3$ or nipalarsite $Ni_8Pd_3As_4$ 29,30 – unnamed phases $(Pd,Ni)_5As_2$ and $(Ni,Pd)_5As_2$ or $Ni_7Pd_3As_4$.
No. 27 and 30 – EDS and the rest WDS analyses; 97.26 * – the total includes 0.20 wt% Pt.

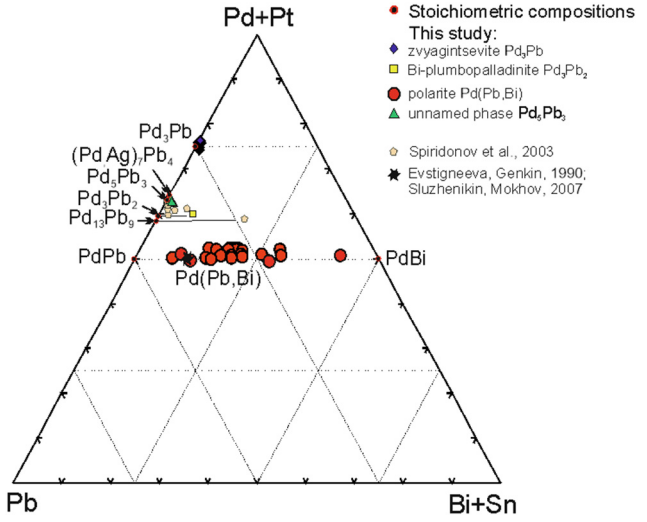

Fig. 12. Compositions of PGE minerals in the Pd-Pb-Bi system. The dotted line shows the trend of solid solutions between the stoichiometric compositions. Star: the composition of the most Pb-rich polarite from previous studies.

silicate melts (Naldrett, 2004). It is widely accepted that immiscible base-metal-enriched sulphide liquid acts as a scavenger of PGEs in magmatic systems (Barnes et al., 1985). This is consistent with disseminated and vein-disseminated ores of the Southern-2 orebody (FigS. 3b, 16a). The samples of massive sulphides show steeper correlations (−MSS – +MSS trend). This trend is due to the separation of early cumulates (MSS) from the fractionated sulphide liquids (Song et al., 2011; Duran et al., 2017). In contrast, massive ores of Southern-2 orebody show no correlation of S and Cu (PGEs) (Figs. 3b, 16a). There is no MSS trend that reflects subsequent fractionation of chalcophile elements in sulphide liquids. The compositions of the studied ores only correspond to the fractionated part of this trend (Fig. 16a). Samples of disseminated sulphide from the Southern-2 orebody have the same Cu/Pd ratios and could be formed at R factors ranging from 1000 to more than 10,000 as it shown by Duran et al. (2017) for Noril'sk, Talnakh and Kharaelakh, but contain more Pd, similar to massive ores (Fig. 16b). The effect of R-factor assumes the zoning of the ore is due to crystal fractionation of Fe-rich monosulphide solid solution from a sulphide liquid (Barnes et al., 1997). However, there is only a slight increase of pyrrhotite in the lower part of the orebody (Krivolutskaya et al., 2018).

High tenors of Cu, Ni and PGEs and the ratios of PPGE/IPGE more than 4000 suggest a very high degree of melt fractionation and high R-factor (Naldrett, 2004). This could be caused by a huge reservoir of silicate magma, much larger than the observed thickness of the Southern-2 orebody. Cu- and PGE-rich ore probably crystallized from a separate portion of silicate melt containing Cu-rich sulphide melt that fractionated previously in the deep magma chamber (Krivolutskaya et al., 2018). This conclusion is supported by the same composition of massive sulphide ores and disseminated mineralization throughout. The fractionation of Cu-rich sulphide liquid in situ led to a slight increase of pyrrhotite in the lower parts of the lode.

6.2. Conditions of crystallization of sulphide minerals and PGMs

The Fe/Ni ratio in pentlandite reflects the thermodynamic conditions of its formation (Kolonin et al., 2000; Kosyakov et al., 2003). Index k = Ni/(Ni + Fe) in pentlandite from the Southern-2 orebody ranges from 0.48 to 0.68, assuming a wide range of sulphur fugacity in the ore formation (Fig. 17). The most depleted in Ni pentlandite of Southern-2 orebody (k = 0.48–0.50) is characterized by the lowest volatility of sulphur ($lgfS_2$) of –10.5. Such pentlandite probably

Table 8
Composition of minerals in the Pd-Pb-Bi system (wt.%).

No.	Sample	Sn	Bi	Pt	Pd	Pb	Ag	Total	Formula:
1	Yuz/7		10.04	0.28	34.03	55.78		100.03	$Pd_{1.00}(Pb_{0.85}Bi_{0.15})_{1.00}$
2	Yuz/12	0.05	16.91	0.29	33.80	49.81	0.09	100.96	$Pd_{0.99}(Pb_{0.75}Bi_{0.25})_{1.00}$
3	Yuz/12	0.34	17.65	0.21	33.40	48.98	0.17	100.75	$Pd_{0.98}(Pb_{0.74}Bi_{0.26}Sn_{0.01})_{1.00}$
4	Yuz/12	0.38	18.21	0.28	34.35	48.14	0.20	101.56	$(Pd_{1.00}Ag_{0.01})_{1.01}(Pb_{0.72}Bi_{0.27}Sn_{0.01})_{1.00}$
5	Yuz/10	0.15	18.24	0.22	33.33	49.52	0.07	101.53	$Pd_{0.99}(Pb_{0.74}Bi_{0.27})_{1.01}$
6	Yuz/0		18.51	0.24	33.29	47.95	0.16	100.14	$Pd_{0.99}(Pb_{0.73}Bi_{0.28})_{1.01}$
7	Yuz/10	0.23	18.06	0.24	34.73	47.01	0.13	100.39	$Pd_{0.99}(Pb_{0.69}Bi_{0.29}Sn_{0.01})_{0.99}$
8	Yuz/0	0.12	25.83	0.42	32.93	40.44	0.30	100.04	$(Pd_{0.98}Pt_{0.01}\ Ag_{0.01})_{1.00}(Pb_{0.62}Bi_{0.38})_{1.00}$
9	Yuz/0		28.42	0.31	33.07	38.73	0.32	100.85	$(Pd_{0.97}Ag_{0.01})_{0.98}(Pb_{0.59}Bi_{0.43})_{1.02}$
10	yuz/11		33.93	0.30	34.54	31.16		99.93	$Pd_{1.02}(Bi_{0.51}Pb_{0.47})_{0.98}$
11	yuz/10		38.60	0.26	35.44	25.81		100.03	$Pd_{1.03}(Bi_{0.57}Pb_{0.39})_{0.96}$
12	yuz/10		39.65		34.35	26.19		100.21	$Pd_{1.01}(Bi_{0.59}Pb_{0.40})_{0.99}$
13	Yuz/10	0.32	52.88	1.58	35.12	10.13	0.81	100.83	$(Pd_{1.02}Pt_{0.02}\ Ag_{0.02})_{1.06}(Bi_{0.78}Pb_{0.15}Sn_{0.01})_{0.94}$
14	Yuz/11	0.50			59.41	40.10		100.00	$Pd_{2.95}(Pb_{1.02}Sn_{0.02})_{1.04}$
15	Yuz/11	0.32			59.83	40.47	0.08	100.69	$Pd_{2.95}(Pb_{1.03}Sn_{0.01})_{1.04}$
16	Yuz/0				59.89	40.61		100.49	$Pd_{2.97}Pb_{1.03}$
17	Yuz/0	0.07			59.94	40.61		100.62	$Pd_{2.97}Pb_{1.03}$
18	Yuz/0	1.75	6.27	0.26	43.92	47.04		99.24	$(Pd_{3.01}Pt_{0.01})_{3.02}(Pb_{1.65}Bi_{0.22}Sn_{0.11})_{1.98}$
19	Yuz/12	0.00	9.22	0.30	43.25	46.17		98.94	$(Pd_{3.00}Pt_{0.01})_{3.01}(Pb_{1.65}Bi_{0.33})_{1.99}$
20	Yuz/10	0.58	1.24		43.52	52.55	2.77	100.67	$(Pd_{4.68}Ag_{0.29})_{4.97}(Pb_{2.90}Bi_{0.07}Sn_{0.06})_{3.03}$
21	Yuz/10	0.46	0.26		43.45	53.42	2.87	100.47	$(Pd_{4.68}Ag_{0.31})_{4.99}(Pb_{2.95}Sn_{0.04}Bi_{0.01})_{3.00}$
22	Yuz/10	0.50	0.25		43.31	53.62	2.97	100.66	$(Pd_{4.66}Ag_{0.32})_{4.98}(Pb_{2.96}Sn_{0.05}Bi_{0.01})_{3.02}$
23	Yuz/10	0.37	0.33		43.48	53.33	2.86	100.36	$(Pd_{4.69}Ag_{0.30})_{4.99}(Pb_{2.95}Sn_{0.04}Bi_{0.02})_{3.01}$
24	Yuz/10	1.09	0.09		44.09	52.54	2.89	100.70	$(Pd_{4.71}Ag_{0.30})_{5.01}(Pb_{2.88}Sn_{0.10})_{2.98}$
25	Yuz/10	0.77	0.23		43.50	53.05	3.00	100.55	$(Pd_{4.67}Ag_{0.32})_{4.99}(Pb_{2.92}Sn_{0.07}Bi_{0.01})_{3.00}$
26	Yuz/11	0.65	0.16		43.63	52.33	2.90	99.67	$(Pd_{4.72}Ag_{0.31})_{5.03}(Pb_{2.90}Sn_{0.06}Bi_{0.01})_{2.97}$
27	Yuz/11	0.57	0.37		43.29	53.41	3.01	100.66	$(Pd_{4.66}Ag_{0.32})_{4.98}(Pb_{2.95}Sn_{0.05}Bi_{0.02})_{3.02}$
28	Yuz/11	0.66	0.26		43.58	52.59	3.05	100.13	$(Pd_{4.69}Ag_{0.32})_{5.01}(Pb_{2.91}Sn_{0.06}Bi_{0.01})_{2.98}$
29	Yuz/11	0.57	0.18		43.58	53.32	3.08	100.73	$(Pd_{4.67}Ag_{0.33})_{5.00}(Pb_{2.94}Sn_{0.05}Bi_{0.01})_{3.00}$
30	Yuz/12	0.61	0.04		43.55	53.24	3.06	100.49	$(Pd_{4.68}Ag_{0.32})_{5.00}(Pb_{2.94}Sn_{0.06})_{3.00}$
31	Yuz/12	0.42	0.15		43.32	53.10	3.09	100.08	$(Pd_{4.68}Ag_{0.33})_{5.01}(Pb_{2.94}Sn_{0.04}Bi_{0.01})_{2.99}$
32	Yuz/12	0.51	0.20		43.70	53.24	2.98	100.63	$(Pd_{4.68}Ag_{0.33})_{5.01}(Pb_{2.94}Sn_{0.04}Bi_{0.01})_{2.99}$

Note. 1–13 − polarite Pd(Pb,Bi) and Pd(Bi,Pb), 14–17 − zvyagintseite Pd_3Pb, 18,19 − plyumbopalladinite $Pd_3(Pb,Bi)_2$, 20–32 − unnamed phase Pd_5Pb_3.

crystallized at temperatures of 560–570 °C (Vaughan and Craig, 1978). According to experimental data in the stability field of pentlandite (Peregoedova, 1999; Kolonin et al., 2000), Ni-rich pentlandite (k = 0.68) could be formed at temperatures of no higher than 500 °C and at $lgfS_2$ no more than –7 (Fig. 17).

According to experiments (Filimonova, 1952), the lamellar intergrowths of cubanite and chalcopyrite are formed at 450 °C and the trellis exolution of chalcopyrite and bornite are formed at 270 °C. Similar textures can form at a temperature of approximately 225 °C, possibly under the influence of mechanical stresses (Ramdohr, 1969).

The five groups (systems) of PGMs were recognized in the Southern-2 orebody: 1) Pt-Fe-Cu-Ni (tetraferroplatinum); 2) Pd-Pt-Cu-Sn (stannopalladinite, rustenburgite, and atokite); 3) Pd-Pb-Bi (zvyagintsevite, plyumbopalladinite, polarite and an unnamed phase Pd_5Pb_2); 4) Pd-Ni-As (majakite, palladoarsenide, stillwaterite, and several unnamed phases), and 5) Au-Pd-Ag-Cu (tetra-auricupride, auricupride, and Au-Ag alloys). All of these minerals were previously documented in the Noril'sk-Talnakh intrusions (e.g., Genkin et al., 1969, 1976, 1981; Kovalenker et al., 1972; Evstigneeva and Genkin, 1990; Distler et al., 1999; Komarova et al., 2002; Kozyrev et al., 2002; Spiridonov et al., 2003, 2004, 2011; Evstigneeva and Trubkin, 2006, 2009, 2010; Sluzhenikin and Mokhov, 2007, 2008, 2015). Nevertheless, the PGMs compositions in Southern-2 orebody are different from those of other deposits of the Noril'sk-Talnakh region because they crystallized from a sulphur- rich, and Cu- and Ni-rich and significantly fractionated sulphide melt.

The Pt-Fe-Cu-Ni alloys of the Talnakh intrusion are different from those of Ural-Alaska-type massifs, as they do not plot on an extended trend from tetraferroplatinum towards tulameenite or ferronickelplatinum. Tetraferroplatinum and tulameenite of Ural-Alaska-type massifs are typically of secondary origin: these minerals replace primary magmatic isoferroplatinum during serpentinization and form rims (Nixon et al., 1990; Cabri and Genkin, 1991; Tolstykh et al., 2015). The ores of the Noril'sk-Talnakh deposits exhibit no such textures. In the studied ores, ferronickelplatinum is part of the evolution of sulphide melt (magmatic origin). The relationships between the minerals of the Southern-2 orebody indicate that the tetraferroplatinum, which is characterized by stable composition and xenomorphic grains (Table 3, Fig. 10), could crystallize from the sulphide melt after stannopalladinite at temperatures between 480 and 300 °C (Bowles, 1990), before the Au-Pd-Cu-Ag alloys. Fig. 17 shows that tetraferroplatinum is stable at low $lgfS_2$. Therefore, pentlandite, which is in equilibrium with tetraferroplatinum, must be relatively iron-rich with k < 0.50 (Fig. 17). However, our data are not consistent with these experiments because samples from the Southern-2 orebody include tetraferroplatinum intergrown with Ni-rich pentlandite (k = 0.67). This discrepancy between the observed textures and the data of lg/S_2 - T°C diagram is difficult to explain at first sight. Ni-rich pentlandite belongs to high-sulphur, but not to low-sulphur association, because the composition of this mineral (Ni/Fe ratio) is positively correlated with sulphur fugacity at the stability of pentlandite (610 °C) (Kullerud, 1962; Kullerud et al., 1969; Vaughan and Craig, 1978). The presence of tetroferroplatinum in this association is most likely due to the reducing conditions in the formation of the Noril'sk-Talnakh ores, which has a much greater effect on the composition of Pt-Fe alloys (Fe enrichment) than sulphur activity (Roeder and Jamieson, 1992). Namely, the reducing conditions are typical during the formation of the Noril'sk-Talnakh ores (Ryabov et al., 2001; Ryabov and Lapkovsky, 2010; Tolstykh et al., 2019).

Stannopalladinite from the Southern-2 orebody is enriched in copper compared to those previously reported (Komarova et al., 2002; Spiridonov et al., 2003). The excessive copper (over one atomic unit) takes the position of Pt in the mineral structure to form $(Pd,Pt,Cu)_5Sn_2Cu$. Experiments in the Pd_3Sn - Cu_3Sn system (Evstigneeva and Nekrasov, 1980) showed an extensive and high-temperature solid solution of $(Pd,Cu)_3Sn$, which crystallizes to form stannopalladinite (Pd_5Sn_2Cu) at 550 °C and taimyrite ($Pd_9Sn_4Cu_3$) at 320 °C

Table 9
Composition of PGE minerals in the Pt-Pd-Cu-Sn system (wt. %).

No	Sample	Pt	Cu	Ni	As	Pb	Bi	Pd	Sn	Total
1	yuz/7	64.68	2.06	1.75				11.57	19.26	99.32
2	yuz/7	60.82	1.46	1.71				14.28	20.03	98.3
3	yuz/7	55.86	1.2	1.18				19.73	21.1	99.07
4	yuz/0	53.82	1.6	1.14				21.73	21.22	99.51
5	yuz/10	24.51	1.08	0.23		0.43	0.15	46.48	24.23	97.11
6	yuz/10	14.64	7.29	0.10	0.23	0.19	0.10	50.43	26.32	99.30
7	yuz/10	9.72	7.45		0.15	0.39	0.53	53.63	26.56	98.43
8	yuz/10	14.36	7.50	0.06	0.20		0.21	49.53	26.22	98.08
9	yuz/10	14.77	7.58	0.12	0.19	0.14		50.38	26.50	99.68
10	yuz/10	13.94	7.65	0.10	0.23			51.64	26.61	100.17
11	yuz/10	13.13	7.79	0.05	0.25		0.30	50.68	26.66	98.86
12	yuz/12	8.14	7.80			0.45	0.37	55.39	26.46	98.61
13	yuz/12	8.03	7.92		0.13	0.24		56.56	27.62	100.50
14	yuz/10	12.63	7.92	0.06	0.26		0.20	50.87	27.14	99.08
15	yuz/12	8.15	7.93	0.07	0.13	0.12	0.10	55.47	27.43	99.40
16	yuz/12	5.65	8.04	0.05	0.14			57.99	28.25	100.12
17	yuz/10	7.57	8.15	0.05	0.24		0.11	56.18	27.17	99.47
18	yuz/12	5.71	8.17		0.18			57.98	27.94	99.98
19	yuz/12	7.18	8.17	0.12	0.14			55.76	27.40	98.77
20	yuz/12	4.87	8.18		0.15			58.56	28.30	100.06
21	yuz/12	6.47	8.24	0.08	0.14		0.09	56.94	28.38	100.34
22	yuz/11	8.84	8.24	0.09	0.22		0.17	54.89	27.19	99.64
23	yuz/12	5.52	8.28		0.17		0.25	59.06	27.31	100.59
24	yuz/12	4.03	8.35		0.16		0.06	59.58	28.29	100.47
25	yuz/12	5.02	8.35		0.14		0.15	58.40	28.23	100.29
26	yuz/11	3.53	8.35		0.22	5.86	0.36	58.47	23.46	100.25
27	yuz/12	4.99	8.39		0.04		0.06	58.23	28.22	99.93
28	yuz/11	6.58	8.41		0.22	1.39	0.41	56.31	26.70	100.02
29	yuz/12	7.41	8.45			4.28	0.42	53.96	23.98	98.50
30	yuz/11	3.86	8.46		0.24	3.62	0.50	58.16	25.09	99.93
31	yuz/12	5.05	8.53		0.14			58.41	28.38	100.51
32	yuz/11	5.90	8.67		0.00		0.19	56.30	27.47	98.53
33	yuz/7	3.38	8.67		0.54	5.94	0.80	57.55	22.54	99.42
34	yuz/10	3.23	8.72		0.23	4.33	0.40	58.91	25.00	100.82
35	yuz/10	5.59	8.80		0.22	2.13	0.23	56.85	26.63	100.45
36	yuz/12	2.89	8.81			1.48	0.34	58.40	26.51	98.43
37	yuz/12	18.51	9.00	0.15	0.11	1.38		45.67	24.18	99.00
38	yuz/12	3.22	9.02		0.24	0.80	0.41	58.18	27.31	99.18
39	yuz/5	2.67	9.05		0.55	1.59	0.89	58.84	24.80	98.39
40	yuz/12	2.65	9.10		0.16	0.40	0.31	59.50	28.17	100.29
41	yuz/11	3.64	9.14		0.22			59.06	28.03	100.09
42	yuz/7	2.67	9.15		0.48	0.10	0.40	58.84	26.77	98.41

1. $(Pt_{1.99}Pd_{0.65}Cu_{0.19}Ni_{0.18})_{3.01}Sn_{0.98}$
2. $(Pt_{1.87}Pd_{0.80}Ni_{0.17}Cu_{0.14})_{2.98}Sn_{1.01}$
3. $(Pt_{1.66}Pd_{1.08}Ni_{0.12}Cu_{0.11})_{2.97}Sn_{1.03}$
4. $(Pt_{1.57}Pd_{1.16}Cu_{0.14}Ni_{0.11})_{2.98}Sn_{1.02}$
5. $(Pd_{2.21}Pt_{0.64}Cu_{0.09}Ni_{0.03})_{2.97}Sn_{1.03}$
6. $(Pd_{4.25}Pt_{0.67}Cu_{0.03}Ni_{0.02})_{4.97}(Sn_{1.99}As_{0.03}Pb_{0.01})_{2.03}Cu_{1.00}$
7. $(Pd_{4.47}Pt_{0.44}Cu_{0.04})_{4.96}(Sn_{1.99}As_{0.02}Pb_{0.02}Bi_{0.02})_{2.04}Cu_{1.00}$
8. $(Pd_{4.22}Pt_{0.67}Cu_{0.07}Ni_{0.01})_{4.96}(Sn_{2.00}As_{0.02}Bi_{0.01})_{2.04}Cu_{1.00}$
9. $(Pd_{4.22}Pt_{0.68}Cu_{0.06}Ni_{0.02})_{4.98}(Sn_{1.99}As_{0.02}Pb_{0.01})_{2.02}Cu_{1.00}$
10. $(Pd_{4.29}Pt_{0.63}Cu_{0.06}Ni_{0.02})_{4.99}(Sn_{1.98}As_{0.03})_{2.01}Cu_{1.00}$
11. $(Pd_{4.25}Pt_{0.60}Cu_{0.09}Ni_{0.01})_{4.95}(Sn_{2.00}As_{0.03}Bi_{0.01})_{2.05}Cu_{1.00}$
12. $(Pd_{4.57}Pt_{0.37}Cu_{0.08})_{5.01}(Sn_{1.96}Pb_{0.02}Bi_{0.02})_{1.99}Cu_{1.00}$
13. $(Pd_{4.56}Pt_{0.35}Cu_{0.07})_{4.98}(Sn_{2.00}As_{0.01}Pb_{0.01})_{2.02}Cu_{1.00}$
14. $(Pd_{4.24}Pt_{0.57}Cu_{0.11}Ni_{0.01})_{4.93}(Sn_{2.03}As_{0.03}Bi_{0.01})_{2.07}Cu_{1.00}$
15. $(Pd_{4.52}Pt_{0.36}Cu_{0.08}Ni_{0.01})_{4.97}(Sn_{2.00}As_{0.02}Pb_{0.01})_{2.03}Cu_{1.00}$
16. $(Pd_{4.63}Pt_{0.25}Cu_{0.08}Ni_{0.01})_{4.96}(Sn_{2.02}As_{0.02})_{2.04}Cu_{1.00}$
17. $(Pd_{4.55}Pt_{0.33}Cu_{0.11}Ni_{0.01})_{5.00}(Sn_{1.97}As_{0.03})_{2.00}Cu_{1.00}$
18. $(Pd_{4.64}Pt_{0.25}Cu_{0.09})_{4.98}(Sn_{2.00}As_{0.02})_{2.02}Cu_{1.00}$
19. $(Pd_{4.54}Pt_{0.32}Cu_{0.11}Ni_{0.02})_{4.99}(Sn_{2.00}As_{0.02})_{2.01}Cu_{1.00}$
20. $(Pd_{4.66}Pt_{0.21}Cu_{0.09})_{4.96}(Sn_{2.02}As_{0.02})_{2.04}Cu_{1.00}$
21. $(Pd_{4.55}Pt_{0.28}Cu_{0.10}Ni_{0.01})_{4.95}(Sn_{2.03}As_{0.02})_{2.05}Cu_{1.00}$
22. $(Pd_{4.46}Pt_{0.39}Cu_{0.12}Ni_{0.01})_{4.99}(Sn_{1.98}As_{0.03}Bi_{0.01})_{2.01}Cu_{1.00}$
23. $(Pd_{4.69}Pt_{0.24}Cu_{0.10})_{5.03}(Sn_{1.94}As_{0.02}Bi_{0.01})_{1.97}Cu_{1.00}$
24. $(Pd_{4.70}Pt_{0.17}Cu_{0.10})_{4.98}(Sn_{2.00}As_{0.02})_{2.02}Cu_{1.00}$
25. $(Pd_{4.64}Pt_{0.22}Cu_{0.11})_{4.97}(Sn_{2.01}As_{0.02}Bi_{0.01})_{2.03}Cu_{1.00}$
26. $(Pd_{4.73}Pt_{0.16}Cu_{0.13})_{5.02}(Sn_{1.70}Pb_{0.24}As_{0.03}Bi_{0.01})_{1.98}Cu_{1.00}$
27. $(Pd_{4.64}Pt_{0.22}Cu_{0.12})_{4.98}Sn_{2.02}Cu_{1.00}$
28. $(Pd_{4.54}Pt_{0.29}Cu_{0.14})_{4.97}(Sn_{1.93}Pb_{0.06}As_{0.03}Bi_{0.02})_{2.03}Cu_{1.00}$
29. $(Pd_{4.49}Pt_{0.34}Cu_{0.18})_{5.01}(Sn_{1.79}Pb_{0.18}Bi_{0.02})_{1.99}Cu_{1.00}$
30. $(Pd_{4.68}Pt_{0.17}Cu_{0.14})_{4.99}(Sn_{1.81}Pb_{0.15}As_{0.03}Bi_{0.02})_{2.01}Cu_{1.00}$
31. $(Pd_{4.62}Pt_{0.22}Cu_{0.13})_{4.97}(Sn_{2.01}As_{0.02})_{2.03}Cu_{1.00}$
32. $(Pd_{4.56}Pt_{0.26}Cu_{0.18})_{5.00}(Sn_{1.99}Bi_{0.01})_{2.00}Cu_{1.00}$
33. $(Pd_{4.68}Cu_{0.18}Pt_{0.15})_{5.01}(Sn_{1.64}Pb_{0.25}As_{0.06}Bi_{0.03})_{1.99}Cu_{1.00}$
34. $(Pd_{4.69}Cu_{0.16}Pt_{0.14})_{5.00}(Sn_{1.78}Pb_{0.18}As_{0.03}Bi_{0.02})_{2.00}Cu_{1.00}$
35. $(Pd_{4.55}Pt_{0.24}Cu_{0.18})_{4.97}(Sn_{1.91}Pb_{0.09}As_{0.02}Bi_{0.01})_{2.03}Cu_{1.00}$
36. $(Pd_{4.70}Cu_{0.19}Pt_{0.13})_{5.01}(Sn_{1.91}Pb_{0.06}Bi_{0.01})_{1.99}Cu_{1.00}$
37. $(Pd5Pt_{0.86}Cu_{0.29}Ni_{0.02})_{5.07}(Sn_{1.85}Pb_{0.06}As_{0.01})_{1.93}Cu_{1.00}$
38. $(Pd_{4.63}Cu_{0.20}Pt_{0.14})_{4.97}(Sn_{1.95}As_{0.03}Pb_{0.03}Bi_{0.02})_{2.03}Cu_{1.00}$
39. $(Pd_{4.72}Cu_{0.22}Pt_{0.12})_{5.05}(Sn_{1.78}Pb_{0.07}As_{0.06}Bi_{0.04})_{1.95}Cu_{1.00}$
40. $(Pd_{4.67}Cu_{0.19}Pt_{0.11})_{4.97}(Sn_{1.98}As_{0.02}Pb_{0.02}Bi_{0.01})_{2.03}Cu_{1.00}$
41. $(Pd_{4.64}Cu_{0.20}Pt_{0.16})_{5.00}(Sn_{1.97}As_{0.02})_{2.00}Cu_{1.00}$
42. $(Pd_{4.68}Cu_{0.22}Pt_{0.12})_{5.02}(Sn_{1.91}As_{0.05}Bi_{0.02})_{1.98}Cu_{1.00}$

Note. 1–4 − rustenburgite $(Pt,Pd)_3Sn$; 5 − atokite $(Pd,Pt)_3Sn$; 6–42 − stannopalladinite Pd_5Sn_2Cu.

under sub-solidus conditions (Fig. 18). Minerals in this study plot between these two end-members and can be products of dissolution (Evstigneeva and Nekrasov, 1980). However, the grains of Cu-rich stannopalladinite appear homogenous under optical and SEM-BSE microscopy (Fig. 10). It could be a stable phase $(Pd,Cu)_5Sn_2Cu$, which formed at 550 °C (Evstigneeva and Nekrasov, 1980) or slightly below, taking into account the excess of Cu, but not < 320 °C. This is consistent with direct crystallization of Pt-Pd-Sn-Cu-Fe compounds from sulphide melt (Kravchenko, 2006).

The Pd-Pb-Bi system has been studied extensively (Mayer et al., 1980; Durussel and Feschotte, 1996; Vymazalová and Drábek, 2011). The most important discovery in this system is an unnamed phase

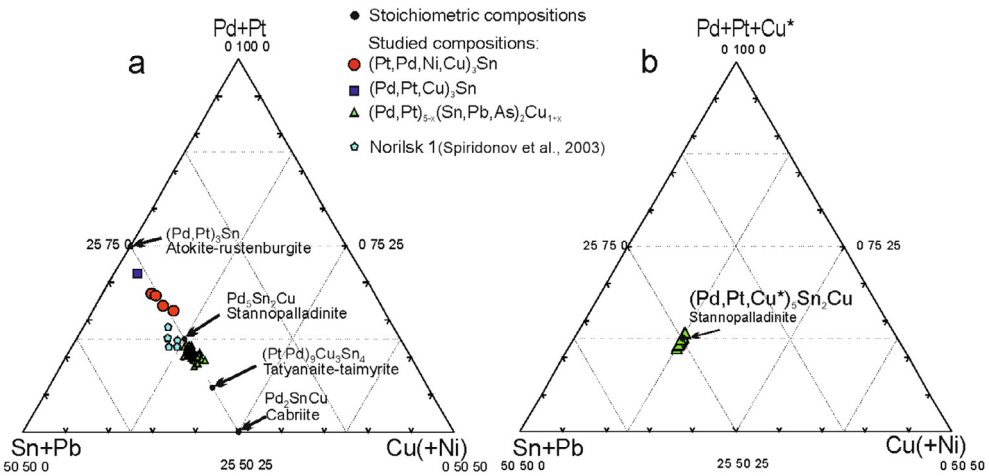

Fig. 13. Compositions of PGE minerals in the (Sn + Pb) − Pd + Pt − Cu(+Ni) system (a) and studied composition of stannopalladinite recalculated to the formula $(Pd,Pt,Cu^*)_5(Sn,Pb)_2Cu$, where Cu* is the excess of Cu over one formula unit.

Pd_5Pb_3, which is present in most samples. The mineral noril'skite $(Pd,Ag)_7Pb_4$ has been described in this system (Vymazalova et al., 2017). The unnamed phase Pd_5Pb_3, like noril'skite, contains ubiquitous Ag (~3 wt%), but upon more accurate calculations based on 5:3 stoichiometry, does not match the formula of noril'skite. The synthetic Pd_5Pb_3 phase has several differences (Mamontov, 1999). The low temperature modification of αPd_5Pb_3 is stable at below of 423 °C. Polarite (PdPb) exists at close conditions (below of 447 °C) (Fig. 19).

The Pd-Ni-As system is represented by seven phases at 450 °C (Makovicky, 2002). Samples from the Southern-2 orebody contain five minerals of this system (Pd_2As, Pd_8As_3, Pd_5As_2, Pd_3As and PdNiAs) (Fig. 11b). Part of these compositions plot outside the stability field of these phases. Most likely, they are thin exsolution textures between adjacent phases, as noted in experiments (Evstigneeva and Trubkin, 2006). The unnamed Pd_5As_2 mineral is common in the Noril'sk ores (Mitenkov et al., 1997; Distler et al., 1999; Komarova et al., 2002) but a feature of the studied assemblage is the presence of Ni-rich analogues of these phase $(Ni,Pd)_5As_2$. An unknown Ni-rich analogue of the stillwaterite $(Ni_{5.86}Pd_{2.19})_{8.05}As_{2.96}$ (Table 7) has been recalculated using the new mineral nipalarsite ($Ni_8Pd_3As_4$) from Monchetundra layered intrusion and was recently approved (Grokhovskaya et al., 2018). It is possible that this unnamed mineral refers to nipalarsite $Ni_{7.98}Pd_{2.99}As_{4.03}$, which was found in the studied association.

The Cu-Au-Pd alloys include CuAu which can be both cuproauride (cubic) and tetra-auricupride (tetragonal). These minerals are stable below the temperatures of 410 °C and 380 °C, respectively (Spiridonov and Pletnev, 2002). Auricupride Cu_3Au is stable below 390 °C (Spiridonov and Pletnev, 2002; Morozov et al., 2013). Intermetallic compounds Cu-Au-Pd, Cu-Au-Ag and Au-Ag alloys from the Southern-2 orebody are formed at a later stage as they occur as rims around previous PGMs (e,g. Fig. 10). The rims of Au-Ag alloys on (Au,Pd)Cu suggest a lower-temperature origin (above 25 °C) (White et al., 1957; Knight and Leitch, 2001).

Sperrylite $PtAs_2$ was not found among the numerous grains of PGM assemblages of Southern-2 orebody and it is a distinctive feature of this locality. In contrast, it is involved in all important phase assemblages across a wide range of temperatures (Makovicky, 2002). In addition, it is the ubiquitous mineral of all types of massive ore described in the Kharaelakh intrusion (Kozyrev et al., 2002) as well in all horizons of the disseminated ore of the Noril'sk 1 intrusion (Komarova et al., 2002). Arsenides and sulfasenides in natural sulphide ores can crystallize from fractionated sulphide melts at temperatures below 900 °C (Bai et al., 2017). However, the solubility of chalcogenides and semi-metals in melts strongly depend on the concentration of Fe. The formation of arsenides and sulfasenides is possible after magma saturation in FeS (Helmy et al., 2017). Sulphide melt was Cu-rich and undersaturated with FeS. Most importantly, crystallization of sperrylite cannot occur during the final stage of sulphide melt fractionation, where it is substantially enriched in Cu (hence not saturated with Fe) (Craig and Kullerud, 1969). It is likely that a high degree of fractionation of sulphide melt and as a consequence, low concentrations of iron is the reason for the absence of sperrylite in the Southern-2 orebody.

The sequence of formation of minerals based on observed texture relationships is: Pt-Pd-Sn (rustenburgite) → Pd-Cu-Sn (stannopalladinite) → Pt-Fe-Cu-Ni (tetraferroplatinum) → Pd-Ni-As (majakite) → Pd-As (palladoarsenide) → Pd-Pb(Bi) (zvyagintsevite and polarite) → Au-Cu-Pd (tetra-auricupride and auricupride) → Au-Ag alloy. Separate fragments of these sequence were found in samples: Pt-Pd-Sn → Pd-Cu-

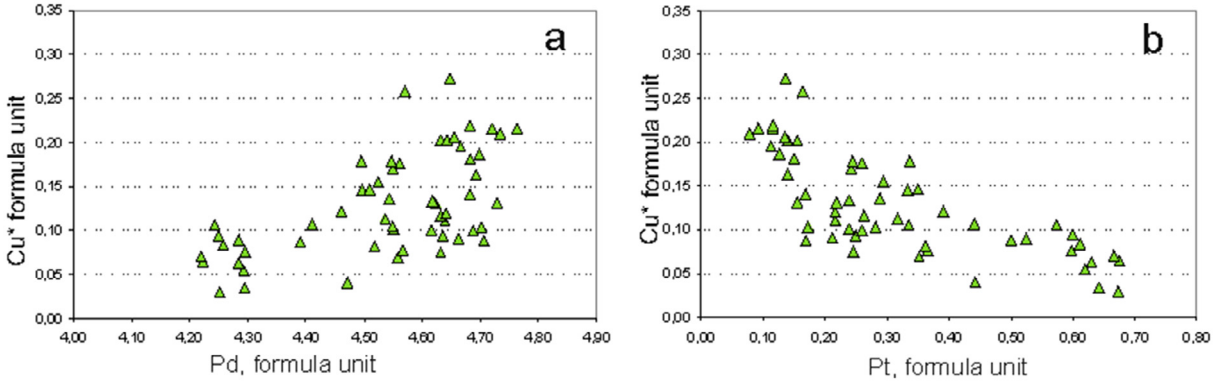

Fig. 14. The contents of Pd vs. Cu* (a) and Pt vs. Cu* (b) in stannopalladinite of Cu* where Cu* is copper excess above one formula unit in stannopalladinite.

Table 10
Composition of the Au-Pd-Cu-Ag alloys (wt.%).

No.	Sample	Cu	Au	Pd	Ag	Total	Formula:
1	yuz/12	50.89	40.15	8.01	0.3	99.35	$Cu_{2.96}(Au_{0.75}Pd_{0.28}Ag_{0.01})_{1.04}$
2	yuz/0	26.37	62.2	9.26	0.21	98.04	$Cu_{1.01}(Au_{0.78}Pd_{0.21})_{0.99}$
3	yuz/0	25.95	63.43	9.21	0.25	98.84	$Cu_{0.99}(Au_{0.79}Pd_{0.21}Ag_{0.01})_{1.01}$
4	yuz/5	26.03	64.78	7.38	0.09	98.28	$Cu_{1.01}(Au_{0.82}Pd_{0.17})_{0.99}$
5	yuz/5	26.17	61.91	9.07	0.24	97.39	$Cu_{1.01}(Au_{0.77}Pd_{0.21Ag0.01})_{0.99}$
6	yuz/7	25.68	64.88	7.54	0.09	98.19	$Cu_{1.00}(Au_{0.82}Pd_{0.18})_{1.00}$
7	yuz/7	25.89	64.12	7.99	0.18	98.18	$Cu_{1.01}(Au_{0.80}Pd_{0.19})_{0.99}$
8	yuz/7	25.64	63.85	8.13	0.28	97.9	$Cu_{1.00}(Au_{0.80}Pd_{0.19})_{1.00}$
9	yuz/7	25.56	64.77	8.32	0.1	98.75	$Cu_{0.99}(Au_{0.82}Pd_{0.19})_{1.02}$
10	yuz/0	0.23	34.09	0.27	65.51	100.1	$Ag_{0.77}Au_{0.22}$
11	yuz/10	0.08	29.35	0.18	69.94	99.55	$Ag_{0.81}Au_{0.19}$
12	yuz/10	0.19	24.55	0.4	74.32	99.46	$Ag_{0.84}Au_{0.15}$
13	yuz/10	0.52	19.15	0.39	79.6	99.66	$Ag_{0.87}Au_{0.11}Cu_{0.01}$
14	yuz/7	0.31	73.02	2.85	22.55	98.73	$Au_{0.61}Ag_{0.34}Pd_{0.04}Cu_{0.01}$
15	yuz/7	0.18	73.81	0.34	24.68	99.01	$Au_{0.61}Ag_{0.38}Cu_{0.01}$
16	yuz/7	0.09	72.44	0.11	25.48	98.12	$Au_{0.61}Ag_{0.39}$
17	yuz/7	1.6	60.31	0.95	36.15	99.01	$Ag_{0.50}Au_{0.45}Cu_{0.04}Pd_{0.01}$

Note: EDS data. 1 – auricupride $Cu_3(Au.Pd)$, 2–9 – tetraauricupride Cu(Au,Pd), 10–17 – Au-Ag alloys.

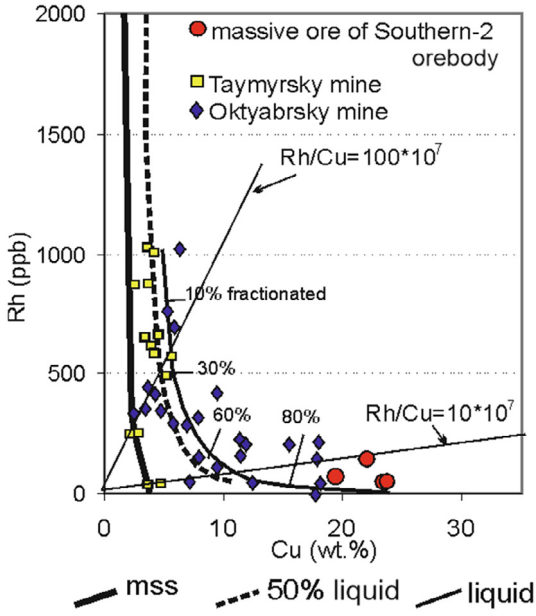

Fig. 15. Diagram of Rh versus Cu for 100% sulphide from the massive ore of Southern-2 orebody. Model curves correspond to Rayleigh fractionation for massive Cu-rich ore (according to Naldrett, 2004).

Sn; Pd-Cu-Sn → Pt-Fe-Cu-Ni → Au-Ag; Pd-Cu-Sn → Pd-Pb(Bi); Pd-Ni-As → Pd-As → Pd-Pb(Bi) → Au-Ag; Pd-Pb(Bi) → Au-Cu-Pd → Au-Ag (Fig. 10). The stability temperatures of individual minerals are given for pure synthetic systems, but it cannot be proved that they are unambiguous. Moreover, natural systems are more complex. Nevertheless, the experimentally determined temperature of sulphide formation and PGM stability are consistent with the established sequence of mineral formation based on the observed textures (Table 11).

6.3. Origin of the massive ores

The atypical geological features of the PGE-Ni-Cu deposits, such as the co-occurrence of huge massive sulphide ores with small size intrusive bodies enriched in PGE, had a significant impact on the development of genetic models for ore formation. Numerous hypotheses (often contradictory) have been proposed for the formation of the sulphide ores mined in the Noril'sk region. These hypotheses include igneous (Godlevsky and Likhachev, 1983; Dyuzhikov et al., 1988; Distler et al., 1988), metasomatic (Zolotukhin, 1997), hydrothermal (Eliseev, 1958), transmagmatic (Marakushev et al, 1998) and pneumatolytic (for PGM) (Spiridonov, 2010) processes for ore formation. Our data support the magmatic model for the formation of the massive ores and are evidenced by quenched solid solutions of sulphides, which were first produced in experiments (Kullerud et al., 1969) and later discovered in the ores (Distler et al., 1996). The magmatic genesis of ores suggests that sulphide melt was either transported by magma from deep chambers and crystallized within a closed magma chamber (Godlevsky,

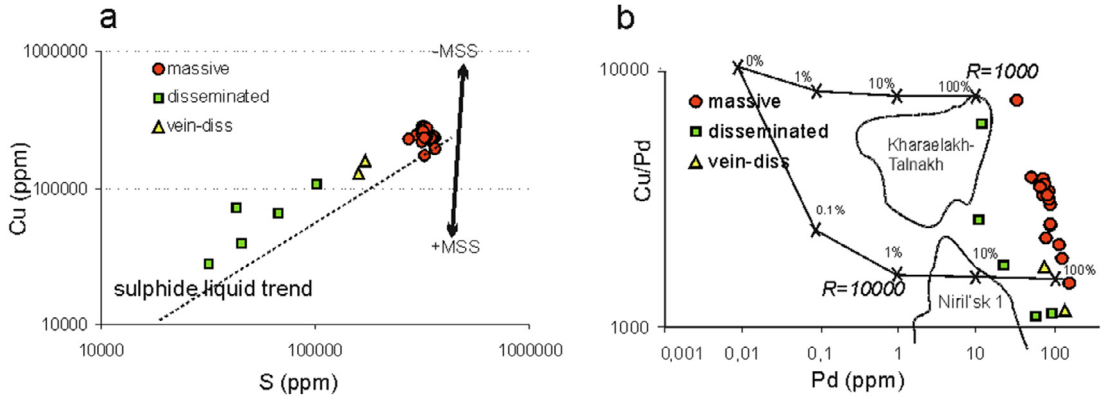

Fig. 16. Diagram of Cu versus S (a) from the different ore types of Southern-2 orebody and Cu/Pd versus Pd (b). MSS trend, modelled compositions of the sulphides at various sulphide percentages, R factors and compositions fields given by (Duran et al., 2017).

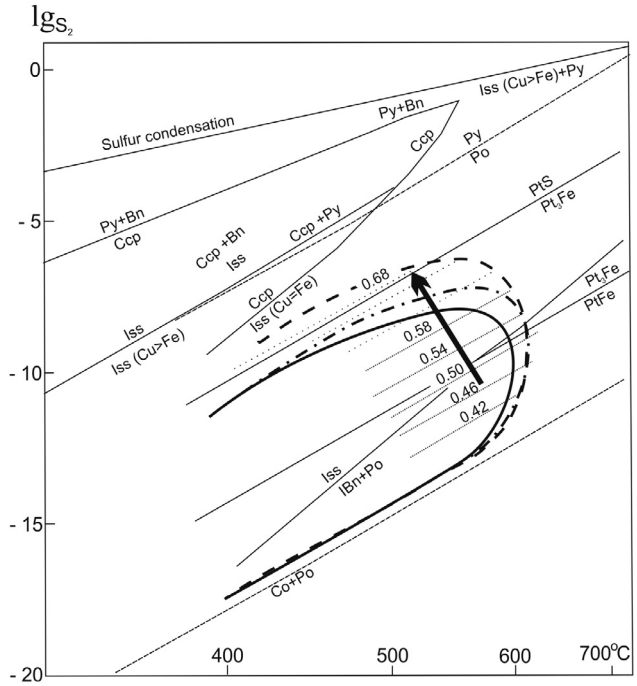

Fig. 17. Physical and chemical conditions of the pentlandite and Pt minerals on a background of the phase equilibria for the Cu − Fe − S and Ni − Fe − S systems (Kolonin et al., 2000). Continuous elliptical curve line − the boundary of the field of stability of pentlandite by Vaughan and Craig (1981), the dotted-dashed curve by Kolonin et al. (2000), and the dotted curve by Peregoedova (1999). The dotted lines within the pentlandite field indicate the changing relationships of Ni/(Ni + Fe) with decreasing temperature and increasing sulphur volatility. The vector indicates the evolution of pentlandite in the massive ores in the Southern-2 orebody.

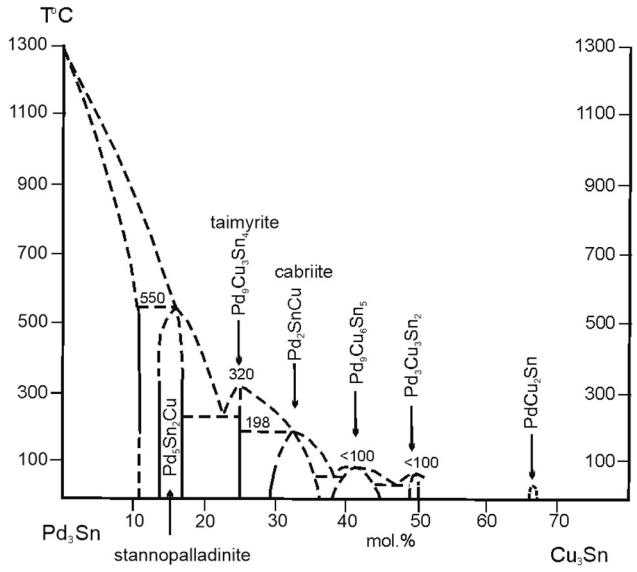

Fig. 18. Phase diagram of the Pd_3Sn − Cu_3Sn system (Evstigneeva and Nekrasov, 1980).

1959; Likhachev, 1965; Genkin et al., 1981; Dyuzhikov et al., 1988; Likhachev, 1973, 2006; Krivolutskaya, 2016; Maier and Groves, 2011; McDonald and Holwell, 2007; Holwell et al., 2014, 2017; Barnes et al., 2016), or was formed in situ within the magma chamber as a result of assimilation of anhydrite-bearing country rocks (Rad'ko, 1991; Naldrett, 1992; Li et al., 2009a, 2009b).

The origin of massive ores is an independent problem in the overall genesis of the Norilsk deposits. In fact, their formation is not directly dependent on the existence of an open or closed magmatic system. Two mechanisms of their formation are assumed: 1) massive ores are the result of filter-pressing when sulphide melt permeated out from the magma chamber into surrounding country rocks during magma crystallization and cooling. In this case, sulphides could be accumulated in the magma chamber in an open system as a result of the assimilation of the host rocks, and in a closed system when they were introduced by magma from depth; 2) intrusion of an independent portion of the sulphide melt and its crystallization after crystallization of the silicate rocks containing interspersed sulphides. In the first scenario, there must be a similarity in composition between disseminated and massive ores, whereas in the second case there is no such similarity. The filter-pressing mechanism (Likhachev, 1996) is possible for the formation of the Southern-2 orebody (Krivolutskaya et al., 2018) because the ores, both disseminated and massive, have a similar and unusual composition (i.e. enriched in PGE and Cu, including the presence of bornite which is not typical of the other Talnakh ore bodies). The model assumes intrusion of silicate melt containing sulphide droplets up to 10 vol% in the modern chamber (Likhachev, 2006). Sulphide melt could also penetrate into the underlying rocks, forming ore bodies in the depressions at the bottom and infill the cracks in them before silicate crystallization ceased (Likhachev, 1996). A review of both open and closed system models, and factors confirming the formation of ores in a closed system was examined in one example from the Oktyabrsky deposit (Krivolutskaya et al., 2019). In addition, the geochemical signature shows a limited amount of host rock assimilation by basaltic melts, as well as a complete absence, which was described in one the example from the Oktyabrsky and Maslovsky deposits (Krivolutskaya et al., 2014).

According to (Distler et al., 1975; Likhachev, 2006), an initially homogenous sulphide melt can fractionate into Fe-rich and Cu-rich melts before crystallization starts. These melts can crystallize either in one chamber, or in separate. In the second case, the Cu-rich liquid was a part of the silicate magma which migrated to the place where the Southern-2 orebody formed. It was colder (1150–850 °C) compared to the Fe-rich liquid (1190–1150 °C) (Likhachev, 2006) and remained in mobile state for longer for it to be driven away to isolated "pockets".

In conditions of increased sulphur fugacity, the evolution of mineral parageneses is: Po(m > h) + Cp + Pn(Fe < Ni) → Cp + Po (m + h) + Pn(Fe < Ni) (Naldrett, 2004). This sequence is in agreement with experimental data on directional crystallization of sulphide melt (Kosyakov et al., 2012) and with the studied ores. This sequence is due to pyrrhotite-chalcopyrite fractionation and is similar to the parageneses of olivine gabbro-dolerite at the bottom rock series of the Noril'sk 1 (Tolstykh et al., 2017). This differs to the evolution of sulphur-poor sulphide melt in which the 'S-deficient' minerals appear (talnakhite, mooihoekite) (Cabri, 1973; Distler et al., 1975; Naldrett, 2004), such as in picritic gabbro-dolerite (Tolstykh et al., 2017).

Our chemical and mineral data from the Southern-2 orebody is consistent with the evolution of the Cu-rich melt. Thus, the chalcopyrite-rich ores of the South-West branch (Southern-2 orebody) and the pyrrhotite-rich ores of the North-East branch of the Talnakh intrusion probably formed from different portions of the sulphide-bearing magma (Krivolutskaya et al., 2018).

7. Conclusions

The ores of the Southern-2 orebody related to the South-Western branch of the Talnakh intrusion possess unique Cu-rich compositions compared to the other deposits of the Noril'sk region. The following geochemical and mineralogical features are due to its generation from a strongly fractionated sulphide melt enriched in Cu, Ni, Pt, Pd, Pb and Au were observed:

1. The ore dominated by chalcopyrite represents the most fractionated

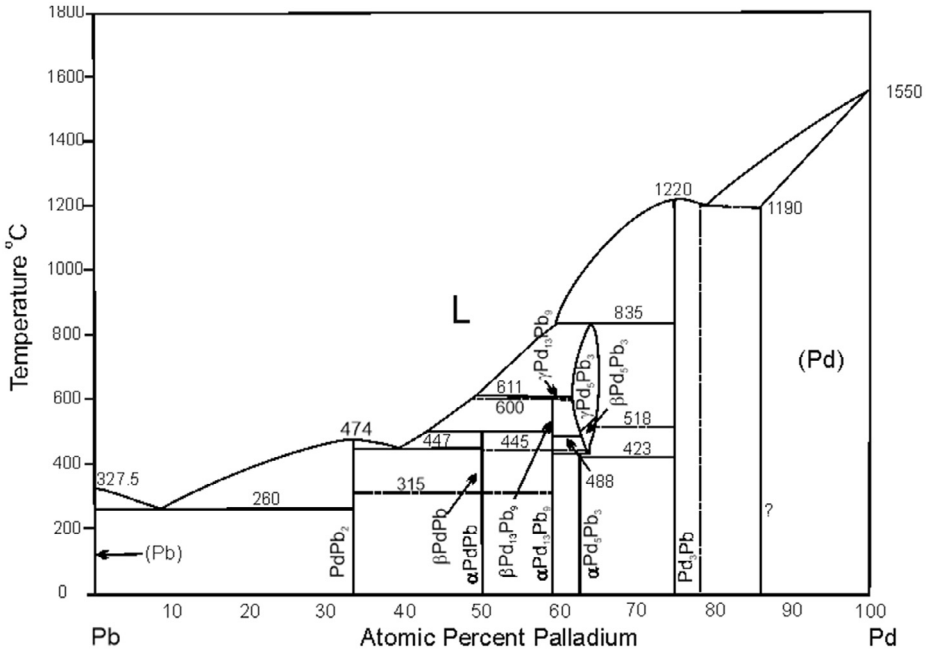

Fig. 19. Phase diagram of the Phase diagram of Pd-Pb alloys (Mamontov, 1999).

Table 11
The crystallization sequence of sulphides and PGM in the Southern-2 Orebody.

Minerals	Temperature, °C
pentlandite	560–500
chalcopyrite	500
cubanite	450
Pd-Cu-Sn (stannopalladinite)	550–320
Pt-Fe-Cu-Ni (tetraferroplatinum)	480–300
Pd-Ni-As (majakite)	450
Pd-As (palladoarsenide)	< 450
Pd-Pb(Bi) (zvyagintsevite, polarite, Pd_5Pb_3)	450–420
Au-Cu-Pd (tetra-auricupride)	410–390
bornite	270–225
Au-Ag alloy	< 390

part of the high-sulphur pyrrhotite-chalcopyrite sequence of formation, unlike other Cu-rich ores consisting of talnakhite and moikhukite of the Oktyabr'sky deposit, which is related to low-sulphur associations.

2. The pyrrhotite ore in the unfractionated part of the sulphide system are absent in the Southern-2 orebody and there is a weak zonation towards increasing pyrrhotite in the lower part of the well section.
3. Ores of the Southern-2 orebody are significantly enriched in PGE, both massive (103.5 ppm) and disseminated (84.4). The ratios of Ni/Cu of both ore types are similar: 0.19 in the massive and 0.21 in the disseminated ores.
4. The chalcopyrite ore is the most fractionated compared to other ores of the Noril'sk region, where the ratio of PPGE/IPGE reaches more then 40000.
5. Studied PGMs are typical for other deposits, but also have the distinctive feature: stanopalladinite is copper-rich, polarite is lead-rich and palladoarsenide is Ni-rich, which is not observed in other ores. In the PGM assemblage there is an abundance of Pt-Fe alloys (tetraferroplatinum) and the absence of sperrylite, which is very common in all the previously studied ores of Noril'sk region.
6. The sulphur fugacity ($lgfS_2$) during formation of pentlandite increased from −10.5 up to −7 for the more Ni-rich pentlandite at temperatures of its stability 560–500 °C. The sequence of crystallization of the PGE minerals was as follows: Pt-Pd-Sn (rustenburgite, atokite) → Pd-Cu-Sn (stannopalladinite) → Pt-Fe-Cu-Ni (tetraferroplatinum) → Pd-Ni-As (majakite) → Pd-As (palladoarsenide) → Pd-Pb(Bi) (zvyagintsevite, polarite and Pd_5Pb_3 unnamed phase) → Au-Cu-Pd (tetra-auricupride and auricupride) → Au-Ag alloy. Experimental data on the PGM system is consistent with this sequence and indicates the formation of PGMs in the temperature range of 550–225 °C.
7. The Southern-2 orebody in the Talnakh intrusion formed most likely due to the process of filter-pressing, i.e. the model of Likhachev (1996, 2006), which provided precipitation of sulphide drops on the bottom of the chamber and penetration of sulphide melts into the country rocks. The Southern-2 orebody formed from the Cu-rich melt, which separated from the Fe-rich melt or MSS before the arrival into the chamber of crystallization. This model is supported by the same geochemical composition of disseminated and massive ores.

Declaration of Competing Interest

The authors declare that they have no known competing financial interests or personal relationships that could have appeared to influence the work reported in this paper.

Acknowledgments

The authors are heartily grateful to geologists of Noril'sk Geology Ltd. S.G. Snisar and S.P. Erykalov for help with sampling and A. Lebedev, I. Fomin, and E. Krasnova for assistance with field work. We are grateful to analysts T.S. Aysueva, V.N. Vlasov, V.I. Lozhkyn and V.I. Menshikov from the Vinogradov Insitute of Geochemistry SB RAS, I.V. Kubrakova and O.A. Tyutyunnik from the Vernadsky Institute of Geochemistry and Analytical chemistry of RAS and N.S. Karmanov from the VS Sobolev Institute of Geology and Mineralogy SB RAS for providing quality analyzes of ores and minerals. The authors express special gratitude to the numerous reviewers who made comments, the work on which significantly improved the manuscript.

The studies were carried out within the framework of the state assignment of the VS Sobolev Institute of Geology and Mineralogy of Siberian Branch of Russian Academy of Sciences financed by Ministry of Science and Higher Education of the Russian Federation. Financial

assistance from the Russian Foundation of Basic Research (https://www.rfbr.ru/rffi/ru/), projects No. 19-35-90033, 19-05-00181) and Russian Science Foundation (https://rscf.ru/), project No. 18-05-70094).

Appendix A. Supplementary data

Supplementary data to this article can be found online at https://doi.org/10.1016/j.oregeorev.2020.103525.

References

Bai, L., Barnes, S.-J., Baker, D.R., 2017. Sperrylite saturation in magmatic sulphide melts: implications for formation of PGE-bearing arsenides and sulfarsenides. Am. Mineralogist. 102 (5), 966–974.

Barkov, A., Martin, R., Poirier, G., Tarkian, M., Pakhomovskii, Y., Men'shikov, Y., 2000a. Tatyanaite, a new platinum-group mineral, the Pt analogue of taimyrite, from the Noril'sk complex (northern Siberia, Russia). Eur. J. Mineral. 12, 391–396.

Barkov, A., Martin, R., Poirier, G., Yakovlev, Y., 2000b. The taimyrite-tatyanaite series and zoning in intermetallic compounds of Pt, Pd, Cu, and Sn from Noril'sk, Siberia, Russia. Can. Mineral. 38, 599–609.

Barkov, A.Y., Martin, R.F., Pakhomovsky, Y.A., Tolstykh, N.D., Krivenko, A.P., 2002. Menshikovite, $Pd_3Ni_2As_3$, a new platinum-group mineral species from Two Layered complexes, Russia. Can. Mineral. 40, 679–692.

Barnes, S.J., Cruden, A.R., Arndt, N.T., Saumur, B.M., 2016. The mineral system approach applied to magmatic Ni-Cu-PGE sulphide deposits. Ore Geol. Rev. 76, 296–316.

Barnes, S.-J., Boyd, R., Korneliussen, A., Nilsson, L.-P., Often, M., Pedersen, R.B., Robins, B., 1988. The use of mantle normalization and metal ratios in discriminating between the effects of partial melting, crystal fractionation and sulphide segregation on platinum-group elements, gold, nickel and copper: examples from Norway. In: Pritchard, H.M., Pott, P.J., Bowles, J.F.W., Cribb, S.J. (Eds.), Geo Platinum 87. Elsevier, London, pp. 113–143.

Barnes, S-J., Lightfoot, P.C., 2005. Formation of magmatic nickel-sulphide ore deposits and processses affecting their copper and platinum-group element contents. In: Hedenquist, J.W., Thompson, J.F.H., Goldfarb, R.J., Richards, J.P. (Eds.), Econ. Geol. 100th Anniversary Volume, pp. 179–213.

Barnes, S.-J., Makovicky, L., Makovicky, M., Rose-Hansen, J., Karup-Moller, S., 1997. Partition coefficients for Ni, Cu, Pd, Pt, Rh, and Ir between monosulphide solid solution and sulphide liquid and the formation of compositionally zoned Ni–Cu sulphide bodies by fractional crystallization of sulphide liquid. Can. J. Earth Sci. 34 (4), 366–374.

Barnes, S.-J., Naldrett, A.J., Gorton, M.P., 1985. The origin of the fractionation of platinum-group elements in terrestrial magmas. Chem. Geol. 53, 303–323.

Barnes, Sarah-Jane, Ripley, Edward M., 2016. Highly siderophile and strongly chalcophile elements in magmatic ore deposits. Rev. Mineral. Geochem. 81 (1), 725–774. https://doi.org/10.2138/rmg.2016.81.12.

Begizov, V.D., Meschankina, V.I., Dubakina, L.S., 1974. Palladoarsenide Pd_2As - the new native palladium arsenide from the copper-nickel ores of Oktyabr'sky deposit. Zapiski VMO CII 1, 104–107 (in Russian).

Bowles, J.F.W., 1990. Platinum-iron alloys, their structural and magnetic characteristics in relation to hydrothermal and low-temperature genesis. Miner. Petrol. 43 (1), 37–47.

Cabri, L.J., 1973. New data on phase relations in the Cu-Fe-S system. Econ. Geol. 68, 443–454.

Cabri, L.J., 2002. The platinum-group minerals. In: Cabri, L.J. (Ed.), The Geology, Geochemistry, Mineralogy and Mineral Beneficiation of Platinum-Group Element. Canadian Institute of Mining. Metallurgy and Petroleum, Special Volume 54, pp. 13–129.

Cabri, L.J., Genkin, A.D., 1991. Re-examination of Pt-alloys from lodes and placer deposits, Urals. Can. Mineral. 29, 419–425.

Cabri, L.J., Laflamme, J.H.G., Stewart, J.M., Rowland, J.E., Chen, T.T., 1975. New data on some palladium arsenides and antimonides. Can. Mineral. 13, 321–335.

Cook, N.J., Ciobanu, C.L., Merkle, R.K.W., Bernhardt, H.-J., 2002. Sobolevskite, taimyrite, and Pt_2CuFe (tulameenite?) in complex massive Talnakhite ore, Noril'sk ore field, Russia. Can. Mineral. 40, 329–340.

Craig, J. R., Kullerud, G., 1969. Phase relations in the Cu-Fe-Ni-S system and their application to magmatic. In: Wilson, H.D.B. (Ed.), Ore Deposits Society of Exploration Geophysicists Geophysical Monograph Series 4, pp. 344–358.

Distler, V.V., Genkin, A.D., Filimonova, A.A., Hitrov, V.G., Laputina, I.P., 1975. The zoning of copper-nickel ores of Talnakh and Oktyabr'sky deposits. Geol. Ore Deposit 2, 16–27 (in Russian).

Distler, V.V., Grokhovskaya, T.L., Evstigneeva, T.L., Sluzhenikin, S.F., Filimonova, A.A., Dyuzhikov, O.A., 1988. Petrology of Magmatic Sulphide Ore Formation. Nauka, Moscow (in Russian).

Distler, V.V., Kulakov, A.A., Sluzhenikin, S.F., Laputina, I.P., 1996. Quenched sulphide solid solutions in Noril'sk ores. Geol. Ore Deposit 38 (1), 41–53 (in Russian).

Distler, V.V., Kunilov, V.E., 1994. Geology and Ore Deposits of the Noril'sk region. Guidebook of 7th International platinum symposium. Moscow-Noril'sk (in Russian).

Distler, V.V., Sluzhenikin, S.F., Cabri, L.J., Krivolutskaya, N.A., Turovtsev, D.M., Golovanova, T.I., Mokhov, A.V., Knauf, V.V., Oleshkevich, O.I., 1999. The platinum ore of the Noril'sk layered intrusions: the ratio of magmatic and fluid concentration of noble metals. Geol. Ore Deposit 41 (3), 241–265 (in Russian).

Dodin, D.A., Batuev, B.N., Mitenkov, G.A., Izoitko, V.M., 1971. Atlas of the Rocks and Ores of the Noril'sk Copper-Nickel deposits. Nedra, Leningrad (in Russian).

Dodin, D.A., Sluzhenikin, S.F., Bogomolov, M.A., 2009. Ores and minerals of the Noril'sk region. The Studio "Polar Star", Moscow (in Russian).

Duran, C.J., Barnes, S.-J., Plese, P., Prasek, M.K., Zientek, M.L., Page, P., 2017. Fractional crystallization-induced variations in sulphides from the Noril'sk-Talnakh mining district (polar Siberia, Russia). Ore Geol. Rev. 90, 326–351.

Durussel, Ph., Feschotte, P., 1996. The binary system Pb–Pd. J. Alloy. Compd. 236, 195–202.

Dyuzhikov, O.A., Distler, V.V., Strunin, B.M., Mkrtychyan, A.K., Sherman, M.L., Sluzhenikin, S.F., Lurye, A.M., 1988. Geology and ore potential of the Noril'sk Ore District. Nauka, Moscow (in Russian). Translated. 1992. Geology and metallogeny of sulphide deposits Noril'sk region USSR. Econ Geol. Monogr 1. Ontario, Spec. Volume. 241.

Eliseev, N.A., 1958. Genesis of Cu-Ni sulphide deposits. Vestnik LGU. 4, 5–16 (in Russian).

Evstigneeva, T.L., Genkin, A.D., 1983. Cabriite Pd_2SnCu, a new species in the mineral group of palladium, tin and copper compounds. Can. Mineral. 21 (3), 481–487.

Evstigneeva, T.L., Genkin, A.D., 1990. Some questions of nomenclature of minerals of platinum metals of copper-nickel sulphide ores. Zapiski VMO XCVIII 6, 708–715 (in Russian).

Evstigneeva, T.L., Nekrasov, I.J., 1980. The conditions of the synthesis phase, and phase relationships in systems Pd_3Sn-Cu_3Sn and Pd-Sn-Cu-HCl. Essays Phys. Chem. Petrol. 9, 20–34 (in Russian).

Evstigneeva, T.L., Trubkin, N.V., 2006. New data on compounds in the Pd2As-Ni2As. Bulletin of the Department of Earth Sciences of Russian Academy of Sciences (electronic scientific and information journal) 1 (24), ISSN 1819-6586 (in Russian).

Evstigneeva, T.L., Trubkin, N.V., 2009. Peculiarities of Pd-Pb-Bi system minerals. Goldschmidt Conference Abstracts A346.

Evstigneeva, T.L., Trubkin, N.V., 2010. About plumbopalladinite and mineral phase Pd2Pb. In: Modern Mineralogy: From Theory to Practice. Russian Mineralogical Society RMS DPI 2010-1-19-0 (in Russian).

Filimonova, A.A., 1952. Experiments on heat of bornite-bearing sulphide ores. Proceedings of the Academy of Sciences of the USSR. Geological Series 3, 76–88 (in Russian).

Gablina, I.F., 2008. The sulphides of copper and copper-iron as indicators of conditions of the formation and transformation of ores. Russian Mineralogical Society RMS DPI 2008-2-10-0 (in Russian).

Genkin, A.D., 1968. The minerals of platinum group metals and their associations in the copper-nickel ores of Noril'sk deposits. Nauka, Moscow (in Russian).

Genkin, A.D., Distler, V.V., Gladyshev, G.D., Filimonova, A.A., Evstigneeva, T.L., Kovalenker, V.A., Smirnov, A.V., Grokhovskaya, T.L., 1981. Sulphide copper–nickel ores of the Noril'sk Deposits. Nauka, Moscow (in Russian).

Genkin, A.D., Evstigneeva, T.L., 1986. Associations of platinum-group minerals of the Noril'sk Copper-Nickel sulphide ores. Econ. Geol. 81, 1203–1212.

Genkin, A.D., Evstigneeva, T.L., Troneva, N.V., Vyalsov, L.N., 1976. Majakite PdNiAs – a new mineral of copper-nickel sulphide ores. Zapiski VMO CV 6, 698–703 (in Russian).

Genkin, A.D., Evstigneeva, T.L., Troneva, N.V., Vyalsov, L.N., 1969. Polarite Pd(Pb, Bi) – a new mineral of copper-nickel sulphide ores. Zapiski VMO XCVIII 6, 708–715 (in Russian).

Genkin, A.D., Muravyova, I.V., Troneva, N.V., 1966. Zvyagintsevite, the natural intermetallic composition of palladium, platinum, lead and tin. Geol. Ore Deposit 8 (1), 94–100 (in Russian).

Gervilla, F., Makovicky, E., Makovicky, M., Rose-Hansen, J., 1994. The system Pd-Ni-As at 790°C and 450°C. Econ. Geol. 89, 1630–1639.

Godlevsky, M.N., 1959. Traps and ore-bearing intrusions of the Noril'sk region. Gostekhizdat, Moscow (in Russian).

Godlevsky, M.N., Likhachev, A.L., 1983. Copper-nickel mineralization in the Noril'sk region. In: Genetic Models of Endogenous Ore Formations. Novosibirsk: Science I, pp. 47–54 (in Russian).

Godovikov, A.A., 1997. Structural-chemical systematic of minerals. Moscow (in Russian).

Grokhovskaya, T., Karimova, O., Vymazalová, A., Laufek, F., Chareev, D., Rassulov, V., 2018. Nipalarsite, IMA 2018-075. CNMNC Newsletter No. 46, December 2018, Mineralogical Magazine, 82.

Helmy, H.M., 2004. Cu-Ni-PGE mineralization in the Genina mafic-ultramafic intrusion, Eastern Desert, Egypt. Can. Mineral. 42, 351–370.

Helmy, H.M., Ballhaus, C., Wohlgemuth-Ueberwasser, C., Fonseca, R., Lauren, V., 2017. Partitioning of Se, As, Sb, Te and Bi between monosulfide solid solution and sulfide melt – application to magmatic sulfide deposits. Geochim. Cosmochim. Acta 74 (21), 6174–6179.

Holwell, D.A., Keays, R.R., Firth, E.A., Findlay, J., 2014. Geochemistry and mineralogy of platinum-group element mineralisation in the River Valley intrusion, Ontario, Canada: a model for early stage S saturation and multi stage emplacement and the implications for 'contact-type' Ni-Cu-PGE mineralization. Econ. Geol. 109, 689–712.

Holwell, D.A., Mitchell, C.L., Howe, G.A., Evans, D.M., Ward, K.A., Friedman, R., 2017. The Munali Ni sulphide deposit, southern Zambia: a multi-stage, mafic-ultramafic, magmatic sulphide-magnetite-apatite-carbonate megabreccia. Ore Geol. Rev. 90, 553–575.

Knight, J., Leitch, C.H.B., 2001. Phase relations in the system Au-Cu-Ag at low temperatures, based on natural assemblages. Can. Mineral. 39, 889–905.

Kolonin, G.R., Orsoev, D.A., Sinyakova, E.F., Kislov, E.V., 2000. Using the ratio Ni: Fe in pentlandite to assess the volatility in the formation of sulphur-containing PGE sulphide mineralization of the Yoko-Dovyren massif. Rep. Russ. Acad. Sci. (Doklady RAN) 370 (1), 87–91 (in Russian).

Komarova, M.Z., Kozyrev, S.M., Simonov, O.N., Lyul'ko, V.A., 2002. The PGE

mineralization of disseminated sulphide ores of the Noril'sk-Taimyr Region. The Geology, Geochemistry, Mineralogy and Mineral Beneficiation of Platinum-Group Elements. In: Cabri L.J. (Ed). Special vol. 54. Canadian Institute of Mining, Metallutry and Petroleum, pp. 547–567.

Korolyuk, V.N., Usova, L.V., Nigmatulina, E.N., 2009. On the accuracy of determining composition of principal rock-forming silicates and oxides with a Jeol JXA-8100 electron microprobe. J. Anal. Chem. 64 (10), 1070–1074.

Kosyakov, F.I., Sinyakova, E.F., Distler, V.V., 2012. Experimental simulation of phase relationships and zoning of magmatic nickel-copper sulphide ores. Russ. Geol. Ore Deposits 54 (3), 179–208.

Kosyakov, V.I., Sinyakova, E.F., Shestakov, V.A., 2003. The dependence of fugacity of sulphur from the composition of phase associations of Fe-FeS-NiS-Ni at 873°K. Geochemistry 7, 730–740 (in Russian).

Kovalenker, V.A., Laputina, I.P., Vyalsov, L.N., Genkin, A.D., Evstigneeva, T.L., 1972. Tellurium minerals in the sulphide copper-nickel ores of the Talnakh and Oktyabr'sky deposits (Noril'sk region). Proceedings of the Academy of Sciences of the USSR, geological series 1, 85–97 (in Russian).

Kozyrev, S.M., Komarova, M.Z., Emelina, L.N., 2002. The mineralogy and behavior of PGM during processing of the Noril'sk-Talnakh PGE-Cu-Ni ores. The Geology, Geochemistry, Mineralogy and Mineral Beneficiation of Platinum-Group Elements. In: Cabri L.J. (Ed). Special vol. 54. Canadian Institute of Mining, Metallutry and Petroleum, pp. 757–791.

Kravchenko, T.A., 2006. Experimental research of features of crystallization of Pt-Pd intermetallic compounds from Cu-Fe sulphide melt. Bulletin of the department of earth sciences (electronic scientific information journal) 1 (24) (in Russian).

Krivolutskaya, N.A., Rudakova, A.V., 2009. Structure and geochemical characteristics of trap rocks from the Noril'sk trough, northwestern Siberian craton. Geochem. Int. 47 (7), 635–656.

Krivolutskaya, N.A., 2014. The evolution of trap magmatism and Pt-Cu-Ni mineralization in the Noril'sk area. The Association of scientific publications KMK, Moscow (in Russian).

Krivolutskaya, N.A., 2016. Siberian traps and Pt-Cu-Ni deposits in the Noril'sk area. Springer international Publishing, Switzerland.

Krivolutskaya, N.A., Plechova, A.A., Kostitsyn, Yu.A., Belyatsky, B.V., Roshchina, I.A., Svirskaya, N.M., Kononkova, N.N., 2014. Geochemical aspects of assimilation by basaltic melts of host rocks during the formation of Noril'sk copper-nickel ores. Petrology 22 (2), 147–170 (in Russian).

Krivolutskaya, N.A., Sobolev, A.V., Snisar, S.G., Gongalskiy, B.I., Hauff, B., Kuzmin, D.V., Tushentsova, I.N., Svirskaya, N.M., Kononkova, N.N., Schlychkova, T.B., 2012. Mineralogy, geochemistry and stratigraphy of the Maslovsky Pt–Cu–Ni sulphide deposit, Noril'sk Region, Russia: implications for relationship of ore-bearing intrusions and lavas. Miner. Deposita 47, 69–88.

Krivolutskaya, N.A., Tolstykh, N.D., Kedrovskaya, T.B., Naumov, K.S., Kubrakova, I.V., Tutunnik, O.A., Gongalsky, B.I., Kovalchuk, E.V., Magazina, L.O., Bychkova, Ya.V., 2018. World-class PGE-Cu-Ni Talnakh Deposit: new data on its structure and unique mineralization. Minerals 8 (4), 124. https://doi.org/10.3390/min8040124.

Krivolutskaya, N., Gongalsky, B., Kedrovskaya, T., Kubrakova, I., Tyutyunnik, O., Chikatueva, V., Bychkova, Ya., Kovalchuk, E., Yakushev, A., Kononkova, N., 2019. Geology of the Western Flanks of the Oktyabr'skoe Deposit, Noril'sk District, Russia: evidence of a closed magmatic system. Mineralium Deposita 54, 611–630.

Kullerud, G., 1962. Thermal stability of pentlandite. Can. Mineral. 7, 353–366.

Kullerud, G., Yand, R.A., Moh, G.H., 1969. Phase relationships in the Cu-Fe-S, Cu-Ni-S, and Fe-Ni-S systems. In: Whson, H.D.B. (Ed.), Economic Geology Monograph. Magmatic Ore Deposits 4, pp. 323–343.

Lavrent'ev, Yu., Usova, L., 1994. The new version of CARAT program for quantitative X-ray spectral analysis. J. Anal. Chem. 49 (5), 462–468 (in Russian).

Lavrent'ev, Yu.G., Karmanov, N.S., Usova, L.V., 2015a. Electron-microprobe determination of mineral compositions: microprobe or scanning-electron microscope. Russ. Geol. Geophys. 56 (8), 1154–1161.

Lavrent'ev, YuG., Korolyuk, V.N., Usova, L.V., Nigmatulina, E.N., 2015b. Electron probe microanalysis of rock-forming minerals with a JXA-8100 electron probe microanalyzer. Russ. Geol. Geophys. 56 (10), 1428–1436.

Li, C., Naldrett, A.J., Ripley, E.M., Schmitt, A.K., 2009a. Magmatic anhydrite - sulphide assemblages in plumbing system of the Siberian Traps. Geology 37, 259–262.

Li, C.S., Ripley, E.M., Naldrett, A.J., 2009b. A new genetic model for the giant Ni–Cu-PGE sulphide deposits associated with the Siberian flood basalts. Econ. Geol. 104, 291–301.

Lightfoot, P.C., Keays, R.R., Evans-Lamswood, D., Wheeler, R., 2012. S saturation history of Nain Plutonic Suite mafic intrusions: origin of the Voisey's Bay Ni–Cu–Co sulphide deposit, Labrador, Canada. Miner. Deposita 47 (1), 23–50.

Lightfoot, P.C., Zotov, I.A., 2014. Geological relationships between the intrusions, country rocks and Ni–Cu–PGE sulphides of the Kharealakh Intrusion, Noril'sk region: implications for the role of sulphide differentiation and metasomatism in their genesis. Northwestern Geol. 47, 1–35.

Likhachev, A.P., 1965. The role of leucocratic gabbro in the formation of Noril'sk differentiated intrusions. Izvestiya AN SSSR. Geol. Ser. 12, 50–66 (in Russian).

Likhachev, A.P., 1973. Experimental study of paragenetic associations in Cu-Fe-S system. Minerals and paragenetic associations of ore deposits, Nauka, Leningrad (in Russian).

Likhachev, A.P., 1994. Ore-bearing intrusions of the Noril'sk Region. Proceeding of the Sudbury–Noril'sk symposium, Ontario. Geol. Surv. Spec. 5, 185–201.

Likhachev, A.P., 1996. Emplacement dynamics of the Talnakh ore-bearing intrusions and related PGM–Cu–Ni ores. Domestic Geol. (Otechestvennaya Geologiya) 8, 20–26 (in Russian).

Likhachev, A.P., 2006. Platinum-copper-nickel and platinum deposits. Eslan, Moscow (in Russian).

Maier, W.D., Barnes, S.-J., Chinyepi, G., Barton, J.M., Eglington, B., Setshedi, I., 2008. The composition of magmatic Ni-Cu-(PGE) sulphide deposits in the Tati and Selebi-Phikwe belts of eastern Botswana. Miner. Deposita 43, 37–60.

Maier, W.D., Barnes, S.-J., De Waal, S.A., 1998. Exploration for magmatic Ni-Cu-PGE sulphide deposits: a review of recent advances in the use of geochemical tools, and their application to some South African ores. S. Afr. J. Geol. 101 (3), 237–253.

Maier, W.J., Groves, D.I., 2011. Temporal and spatial controls on the formation of magmatic PGE and Ni–Cu deposits. Miner. Deposita 46, 841–857.

Makovicky, E., 2002. Ternary and quaternary phase systems with PGE. In: Cabri, L.J. (Ed), The Geology, Geochemistry, Mineralogy and Mineral Beneficiation of Platinum-Group Elements. Special vol. 54. Canadian Institute of Mining, Metallutry and Petroleum, pp. 131–175.

Mamontov, M.N., 1999. Thermodynamic analysis of phase equilibria in the Pb-Pd system. Bull. Moscow Univ. Ser. 2 Chem. 40 (4), 223–228 (in Russian).

Marakushev, A.A., Paneyakh, N.A., Rusinov, V.L., Pertsev, N.N., Zotov, I.A., 1998. Petrological models of giant ore deposits. Geol. Ore Deposit 40, 236–255.

Mayer, H.W., Ellner, M., Schubert, K., 1980. Crystal structure of $Pd_{13}Pb_9$. Less Common Metals 71 (2), 28–38.

McDonald, I., Holwell, D.A., 2007. Did lower zone magma conduits store PGE-rich sulphides that were later supplied to the Platreef. S. Afr. J. Geol. 110, 611–616.

Men'shikov, V.N., Vlasov, V.I., Lozhkyn, V.N., Sokolnikova, Yu.V., 2016. Determination of platinum-group elements in rocks by ICP-MS with the external grading after the separation of the matrix elements on the KU-2-8 cation exchanger. Anal. Control 20 (3), 190–201 (in Russian).

Mitenkov, G.A., Knauf, V.V., Yertseva, L.N., Emelina, L.N., Kunilov, V.E. Stekhin, A.I., Oleshkevich, O.I., Yatsenko, A.A., Alekseyeva, L.I., 1997. Minerals of platinum-group elements in massive pyrrhotite ores of Talnakh. In: The Main Problems in the Study of Magmatic Ore Deposits. Nauka, Moscow, pp. 284–285 (in Russian).

Morozov, M.M., Markova, T.N., Klopotov, A.A., 2013. Features of structural-phase states in the ternary alloys based on PdCu system. Bull. Siberian State Indus. Univ. 2 (4), 10–13 (in Russian).

Naldrett, A.J., 1992. Model for the Ni–Cu–PGE ores of the Noril'sk region and its application to other areas of flood basalts. Econ. Geol. 87, 1945–1962.

Naldrett, A.J., 2004. Magmatic Sulphide Deposits: Geology, Geochemistry and Exploration. Springer, Berlin/Heidelberg/New York.

Naldrett, A.J., Fedorenko, V.A., Asif, M., Lin, S., Kunilov, V.E., 1996. Controls on the composition of Ni-Cu sulphide deposits as illustrated by those at Noril'sk, Siberia. Econ. Geol. 91, 751–773.

Nixon, G.T., Cabri, L.J., Laflamme, J.H.G., 1990. Platinum-group element mineralization in lode and placer deposits associated with the Tulameen Alaskan-type complex, British Columbia. Can. Mineral. 28, 503–535.

Peregoedova, A.V., 1999. Physical and chemical behavior of Pt and Pd during crystallization of Fe, Ni, Cu-containing sulphide melts, and in subsequent subsolidus transformations. Author. Dis. of kand. geol.-min. nauk, Novosibirsk (in Russian).

Rad'ko, V.A., 1991. Model of geodynamic differentiation of the intrusive traps of the northwestern Siberian Platform. Geol. Geophys. 11, 19–27 (in Russian).

Rajamani, V., Prewitt, C.T., 1973. Cristal chemistry of natural pentlandites. Can. Mineral. 12 (3), 178–187.

Ramdohr, P., 1969. The Ore Minerals and Their Intergrowths. Pergamon Press, Oxford.

Razin, L.V., Borishanskaya, S.S., 1970. Mineral occurrence forms of platinum metals and gold in disseminated ores of the Noril'sk 1 deposit. Moscow, Proc. TsNIGRI. 87, 28–36 (in Russian).

Roeder, P.L., Jamieson, H.E., 1992. Composition of chromite and co-existing Pt–Fe alloy at magmatic temperatures. Australian J. Earth Sci. 39, 419–426.

Ryabov, V.V., Lapkovsky, A.A., 2010. Native iron (-platinum) ores from the Siberian Platform trap intrusions. Australian J. Earth Sci. 57, 707–736.

Ryabov, V.V., Shevko, A.Ya., Gora, M.P., 2001. Magmatic Formations in Noril'sk region. Volume 1. Trapp Petrology. Nonparel Rublisher, Novosibirsk (in Russian).

Sinyakova, E.F., Kosyakov, V.I., 2009. Experimental modeling of zonality of copper-rich sulphide ores in copper-nickel deposits. Rep. Russ. Acad. Sci. (Doklady RAN) 427 (1), 787–792 (in Russian).

Sluzhenikin, S.F., 2011. Platinum-copper-nickel and platinum ores of Noril'sk region and their ore mineralization. Russ. J. General Chem. 81 (6), 1288–1301.

Sluzhenikin, S.F., Distler, V.V., Dyuzhikov, O.A., Kravtsov, V.F., Kunilov, V.E., Laputina, I.P., Turovtsev, D.M., 1994. Low-sulphide platinum mineralization in the Noril'sk differentiated intrusions. Geol. Ore Deposit 36 (3), 195–217 (in Russian).

Sluzhenikin, S.F., Krivolutskaya, N.A., Rad'ko, V.A., Malitch, K.N., Distler, V.V., Fedorenko, V.A., 2014. Ultramafic-mafic intrusions, volcanic rocks and PGE-Cu-Ni sulphide deposits of the Noril'sk province, Polar Siberia. In: Simonov, O.N. (Ed.), 12th International Platinum Symposium. Field trip guidebook. IGG UB RAS, Yekaterinburg.

Sluzhenikin, S.F., Mokhov, A.V., 2007. Minerals of system PdBi-PdTe-PdSb-PdPb in Pt-Cu-Ni and Pt ores of the Noril'sk region. Ann. Session RMO 119–121 (in Russian).

Sluzhenikin, S.F., Mokhov, A.V., 2008. Natural iron-platinum, palladium-platinum and palladium-copper alloys in platinum-copper-nickel and platinum ores of the Noril'sk deposit. In: Problems of Ore Geology, Mineralogy, Petrology and Geochemistry. Moscow, pp. 346–347 (in Russian).

Sluzhenikin, S.F., Mokhov, A.V., 2015. Gold and silver in PGE–Cu–Ni and PGE ores of the Noril'sk deposits, Russia. Mineral. Deposita 50, 465–492.

Song, X., Wang, Y., Chen, L., 2011. Magmatic Ni-Cu-(PGE) deposits in magma plumbing systems: features, formation and exploration. Geosci. Front. 2 (3), 375–384.

Spiridonov, E.M., 2010. The ore-magmatic system of the Noril'sk ore field. Russ. Geol. Geophys. 51 (9), 1059–1077.

Spiridonov, E.M., Korotaeva, N.N., Kulikova, I.M., Mashkina, A.A., Zhukov, N.N., 2011. Palladoarsenide Pd_2As - a breakdown product of majakite PdNiAs in the Noril'sk sulphide ores. New Data Minerals (Fersman Museum of RAS) 46, 48–54 (in Russian).

Spiridonov, E.M., Kulagov, E.A., Kulikova, I.M., 2003. Platinum and palladium-bearing

tetraauricupride and associated minerals in the ores of the Noril'sk-I deposit. Geol. Ore Deposit 45 (3), 261–271 (in Russian).
Spiridonov, E.M., Kulagov, E.A., Kulikova, I.M., 2004. Association of minerals of palladium, platinum and gold in ores of the Noril'sk deposit. Geol. Ore Deposit 46 (2), 175–192 (in Russian).
Spiridonov, E.M., Pletnev, P.A., 2002. Cuprous gold deposit of Gold Mountain. Nauchniy Mir, Moscow (in Russian).
Stekhin, A.I., 1994. Mineralogical and geochemical characteristics of the Cu-Ni ores of the Oktyabr'sky and Talnakh deposits. Proc. Sudbury-Noril'sk Symp. OGS Special 5, 217–230 (in Russian).
Strunin, B.M., 1991. Geological map of Noril'sk ore region at a scale of 1:200,000, Explanatory note. Geoinformmark, Moscow (in Russian).
Sukhanova, E.N., 1968. Zoning of orebodies, intrusions, and tectono-magmatic clusters and their applied implications. In: Geology and Mineral Resources of the Noril'sk Mining District. NTO Tsvetmet Publishing house, Noril'sk, pp. 139–142 (in Russian).
Tagle, R., Berlin, J., 2008. A database of chondrite analyses including platinum-group elements, Ni Co, Au, and Cr: implications for the identification of chrondritic projectiles. Meteoritics Planetaru Sci. 43 (3), 541–559.
Tolstykh, N., Kozlov, A., Telegin, Yu., 2015. Platinum mineralization of the Svetly Bor and Nizhny Tagil intrusions, Ural Platinum Belt. Ore Geol. Rev. 67, 234–243.
Tolstykh, N.D., Shvedov, G.I., Polonyankin, A.A., Zemlyansky, S.A., 2017. Mineralogical and geochemical feature of the disseminated ores of the southern part of the Noril'sk 1 deposit. IOP Conf. Ser.: Earth Environ. Sci. 110, 1–8.
Tolstykh, N.D., Zhitova, L.M., Shapovalova, M.O., Chayka, I.F., 2019. The evolution of the ore-forming system in the low sulphide horizon of the Noril'sk 1 intrusion, Russia. Mineral. Mag. 83 (5), 673–694.
Tolstykh, N.D., 2008. PGE mineralization in marginal sulphide ores of the Chineisky layered intrusion, Russia. Miner. Petrol. 92, 283–306.
Tolstykh, N.D., Podlipsky, M.Y., 2010. Heavy concentrate halos as prospecting guides for PGE mineralization. Geol. Ore Deposit 52 (3), 196–214.
Urvantsev, N.N., 1972. Some questions on formation of ore-bearing intrusion and ores. In: Cu-Ni Ores of Talnakh Ore Junction. Nedra, Leningrad. pp. 100–144 (in Russian).
Vaughan, D., Craig, J., 1978. Mineral Chemistry of Metal Sulphide. Cambridge University Press Cambridge, London-New York-Melbourne.
Vaughan, D.J., Craig, J.R., 1981. Mineral Chemistry of Metal Sulphides. Izd. Mir, Moscow (in Russian).
Vymazalová, A., Drábek, M., 2011. The system Pd-Pb-Te AT 400°C: phase relations involving pasavaite and potential minerals. Can. Mineral. 49, 1679–1686.
Vymazalova, A., Laufek, F., Sluzhenikin, S.F., Stanley, C.J., 2017. Noril'skite, $(Pd, Ag)_7Pb_4$, a new mineral from Noril'sk-Talnakh deposit, Russia. Mineral. Mag. 81 (3), 531–541.
White, J.L., Orr, R.L., Hultgren, R., 1957. The thermodynamic properties of silver–gold alloys. Acta Metall. 5, 747–760.
Yu, T.-H., Lin, S.-J., Chao, P., Fang, C.-S., Huang, C.-S., 1974. A preliminary study of some new minerals of the platinum group and another associated new one in platinum-bearing intrusions in a region in People's Republic of China. Acta Geol. Sin. 2, 202–218 (in Chinese with English abstract).
Zolotukhin, V.V., 1997. Basaltic Pegmatoides of the Noril'sk Ore-bearing Intrusions and the Problem of Their Origin. Trudy IGG, Novosibirsk (in Russian).